SENSITIZATION OF SOL-GEL DERIVED TITANIA-SILICA PHOTOCATALYTIC THIN FILMS WITH ASCORBIC ACID

A THESIS SUBMITTED TO
THE GRADUATE SCHOOL OF NATURAL AND APPLIED SCIENCES
OF
MIDDLE EAST TECHNICAL UNIVERSITY

BY

EMRE YILMAZ

IN PARTIAL FULFILLMENT OF THE REQUIREMENTS
FOR
THE DEGREE OF MASTER OF SCIENCE
IN
CHEMICAL ENGINEERING

FEBRUARY 2012

Approval of the thesis:

SENSITIZATION OF SOL-GEL DERIVED TITANIA-SILICA PHOTOCATALYTIC THIN FILMS WITH ASCORBIC ACID

submitted by **EMRE YILMAZ** in partial fulfillment of the requirements for the degree of **Master of Science in Chemical Engineering Department, Middle East Technical University** by,

Prof. Dr. Canan Özgen
Dean, Graduate School of **Natural and Applied Sciences** _____

Prof. Dr. Deniz Üner
Head of Department, **Chemical Engineering** _____

Prof. Dr. Gürkan Karakaş
Supervisor, **Chemical Eng. Dept., METU** _____

Examining Committee Members:

Prof. Dr. Timur Doğu
Chemical Engineering Dept., METU _____

Prof. Dr. Gürkan Karakaş
Chemical Engineering Dept., METU _____

Prof. Dr. Çiğdem Güldür
Chemical Engineering Dept., Gazi University _____

Assoc. Prof. Dr. Yusuf Uludağ
Chemical Engineering Dept., METU _____

Assist. Prof. Dr. Halit Levent Hoşgün
Chemical Engineering Dept., Osman Gazi University _____

Date: 10.02.2012

I hereby declare that all information in this document has been obtained and presented in accordance with academic rules and ethical conduct. I also declare that, as required by these rules and conduct, I have fully cited and referenced all material and results that are not original to this work.

Name, Lastname: Emre Yılmaz

Signature:

ABSTRACT

SENSITIZATION OF SOL-GEL DERIVED TITANIA-SILICA PHOTOCATALYTIC THIN FILMS WITH ASCORBIC ACID

Yılmaz, Emre
M. Sc., Department of Chemical Engineering
Supervisor: Prof. Dr. Gürkan Karakaş

January 2012, 68 pages

The photocatalytic activity of semiconductor metal oxides can be improved by the addition of sensitizer which enhances the band gap by considerable red shift of the absorption edge of semiconductor. In the present study, the effect of ascorbic acid as sensitizer on the photocatalytic activity of titania-silica binary mixtures was studied. The SiO_2-TiO_2 mixtures having 50wt%Ti:Si composition were prepared with sol-gel method. The surface area and porosity of the samples were modified by using various amounts of polyethylene glycol (PEG) as template. The thin films of the samples were obtained by dip coating of glass plates to colloidal solutions. The samples were characterized by methylene blue adsorption method and UV-Vis spectrophotometry. The photocatalytic activities of the samples were measured with methylene blue degradation, methyl orange degradation and direct water splitting in the presence and absence of ascorbic acid. Increase in the surface area and reaction rate with increasing PEG addition until a threshold value was observed. Highest methylene blue degradation activity was observed for 27g PEG added sol-gel derived film and surface area of this film is measured as $44 m^2/m^2$. Ascorbic acid presence shows a significant increase in the

photocatalytic degradation activity of methyl orange. The sensitization effect of ascorbic acid was also compared with the effect of EDTA. It was found that the effect of ascorbic acid on the methyl orange degradation rate is significantly higher than the effect of EDTA. However, the effect of EDTA is more pronounced in water splitting reaction.

Keywords: Titanium dioxide, ascorbic acid, photocatalysis, methyl orange, thin film, sensitization

ÖZ

SOL-JEL YÖNTEMİ İLE HAZIRLANMIŞ TİTANYUM DİOKSİT-SİLİKON DİOKSİT FOTOKATALİTİK İNCE FİLMLERİN ASKORBİK ASİT İLE DUYARLILAŞTIRILMASI

Yılmaz, Emre
Yüksek Lisans, Kimya Mühendisliği Bölümü
Tez Yöneticisi: Prof. Dr. Gürkan Karakaş

Ocak 2012, 68 sayfa

Yarı iletken fotokatalizörlerde duyarlılaştırıcı ilavesi ile bant yapısında kırmızıya kayma ve bunun sonucu olarak da analmı bir aktivite artışı gözlemlenir. Bu çalışmada askorbik asitin, titanyum dioksit-silikon dioksit ikili karışımları üzerindeki duyarlılaştırıcı etkisi incelenmiştir. Sol-jel metoduyla kütlece 1:1 Ti:Si oranına sahip olan SiO_2-TiO_2 karışımları hazırlanmıştır. Yüzey alanı ve gözeneklilik çeşitli miktarlarda PEG ilavesi ile ayarlanmıştır. Hazırlanan koloit karışımın cam plakalar üzerine daldırıp-çıkarma yöntemiyle uygulanması sonucu ince film örnekleri hazırlanmıştır. Örnekler metilen mavisi tutunumu ve UV-Vis spektrofotometrisi yöntemleri ile karakterize edilmiştir. Fotokatalitik etkinlik ise metilen mavisi bozunumu, metil turuncusu bozunumu ve suyun doğrudan fotokatalitik hidrolizi deneylerinin askorbik asit varlığında ve yokluğunda uygulanması ile ölçülmüştür. Bir sınır değerine kadar artan PEG ilavesinin yüzey alanı ve aktivetede de artış gösterdiği gözlenmiştir. En yüksek aktivite 27g PEG eklenmiş "sol-jel"den türetilmiş filmde gözlenmiştir. Bu filmin yüzey alanı $44 m^2/m^2$

olarak bulunmuştur. Askorbik asit varlığının film aktivitesi üzerinde olumlu bir etkisi olduğu gözlemlenmiştir. Askorbik asidin etkisi hasaslaştırma etkisi EDTA ile de karşılaştırılmıştır. Güneş simülatörü cihazında gerçekleştirilen metil turuncusu parçalanma deneylerinde askorbik asidin EDTA üzerinde üstünlüğü gözlenmiştir. Ancak UV hücresinde gerçekleştirilen suyun doğrudan hidrolizi deneylerinde EDTA'nın askorbik aside nazaran daha etkin gözlenmiştir.

Anahtar Kelimler: Titanyum dioksit, askorbik asit, fotokatalizör, metil turuncusu, ince film, hassaslaştırma

To my family

ACKNOWLEDGEMENTS

First I would like to thank my supervisor Prof. Dr. Gürkan Karakaş for his academic guidance but especially for his never ending patience and support. He is an understanding and caring boss which I will seek for his guidance in the rest of my life.

I would also like to show my gratitude to Prof. Dr. Deniz Üner, Prof. Dr. H. Önder Özbelge, Assoc. Prof. Dr. Halil Kalıpçılar and Assoc. Prof. Dr. Yusuf Uludağ for their valuable tutorship.

In the period of my M.S. study I also found the chance of assisting Prof. Dr. Timur Doğu and Prof. Dr. Levent Yılmaz in several courses. I learned much from them and would like to thank them as well.

A very particular set of friend including Hasan, Gürkan, Soyadaş, Emir, Akın, Adaş and Caner made my life bearable so far. It is my duty to thank them.

I would also mention two of my friends, Emre Büküşoğlu and Riza Güven Alptekin, without their presence I wouldn't be able to make it this far in chemical engineering.

I also thank to rest of my friends from METU Chemical Engineering Department, especially, Muhlis, Simge, Sena, Eda, Berk, Merve, Ayşegül, Engin and Hasan. Thank you all, for being around me for the past my seven and a half year.

And my group members Merve, Doruk, Beril, Özgen and Pelin whom supported me with a healthy working environment and their friendship should be acknowledged as well.

And lastly I would like to thank ODTU BAP Koordinatorlüğü for their financial support to the project.

TABLE OF CONTENTS

LIST OF TABLES

TABLES

LIST OF FIGURES

FIGURES

CHAPTER 1

INTRODUCTION

Titanium dioxide a metal oxide semiconductor with delicate physical properties which makes it useful in different industries. The use TiO_2 is involved in varies from color industry to electronics, materials and catalysts area. And it is a main corner in nanotechnology.

Titanium dioxide has important photocatalytic applications such as self-cleaning surfaces, water purification, air purification, self-sterilizing surfaces, photocatalytic lithography and water splitting.

Limited surface area of titania catalysts is an important factor affecting catalytic efficiency. In order to overcome this problem, thin films of titanium dioxide and silicon dioxide binary mixtures are examined in this study. Thin film are synthesized by sol gel method and poly ethylene glycol (PEG) is used as molecular template to enhance the porosity and surface area of the films.

The photocatalytic efficiency of metal oxide semiconductor is limited with scarcity of harvested photons, electron hole combination, and back reaction of products (depending on the reaction) for photocatalytic applications, especially for water splitting applications. One of the promising solutions to enhance photocatalytic efficiency is sensitization. In this study ascorbic acid is tested as sensitizer on titania-silica mixed oxide photocatalysts on methyl orange degradation and water splitting reactions.

Ascorbic acid is a powerful antioxidant and can be found in waste streams of several processes in food industry. Positive results of this study may lead to utilization of waste streams in energy production with water splitting applications.

Thin films synthesized with sol-gel method with different PEG additions are compared with respect to relative surface areas. Than the effect of surface area on the photocatalytic reaction is investigated. Later effect of ascorbic acid as a sensitizer is studied. First adsorption of ascorbic acid on film surfaces is studied. Then, the effect of ascorbic acid presence in the reaction medium to photocatalytic activity of the films is studied. The activities of samples were tested for methyl orange degradation by using artificial solar irradiation. At last the effect of ascorbic acid is compared with a well-known hole scavenger ethylenediaminetetraacetic acid (EDTA).

CHAPTER 2

LITERATURE SURVEY

2.1. Titanium Dioxide

Titanium dioxide (titania) is a semiconductor metal oxide which has various applications starting from white pigments in paint industry [1] to optical storage media production [2] and cutting edge electronic devices applications such as memristors [3].

Titania can be found in three different crystal structures in the nature as anatase, rutile and brookite [4]. Crystal lattices for three different forms of titania are illustrated in Figure 2.1 and some physical properties regarding to these different crystal structures are tabulated in Table 2.1. Anatase and rutile phases have 3.2eV and 3.0eV band gaps respectively. The wider band gap of anatase phase of titanium dioxide enables the excitation of the electrons with photons having wavelength smaller than 388nm in UV band of electromagnetic spectrum.

Band gap energies for rutile and anatase phases of titanium dioxide are presented and compared with various semiconductors in

Figure 2.2. Comparison with some selected redox potentials are also presented in the figure.

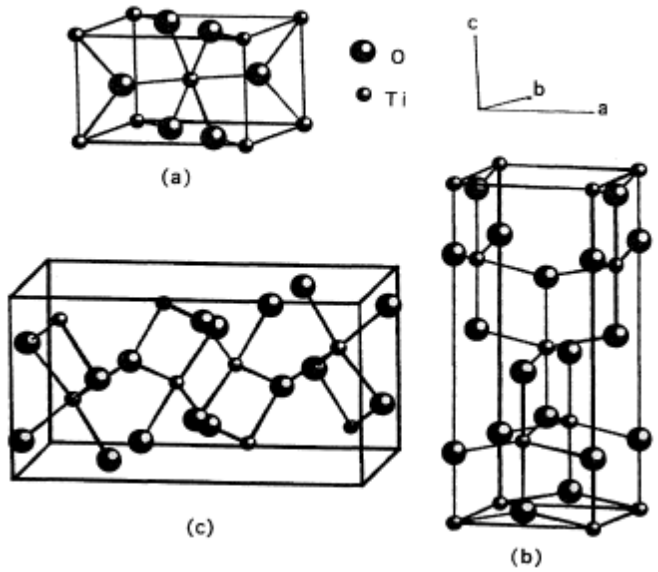

Figure 2.1: Crystal structures of titania (a) Rutile, (b) Anatase and (c) Brookite [5]

Table 2.1: Some physical properties for different crystal structures of titania. [5]

	Rutile	**Anatase**	**Brookite**
Crystal structure	tetragonal	tetragonal	orthorhombic
Lattice constants (Å)	a=4.5936 c=2.9587	a=3.784 c=9.515	a=9.184 b=5.447 c=5.145
Space group	$P4_2/mnm$	$I4_1/amd$	*Pbca*
Molecule/cell	2	4	8
Volume/molecule (Å^3)	31.2160	34.061	32.172
Density (g/cm^3)	4.13	3.79	3.99
Ti-O bond length (Å)	1.949(4) 1.980(2)	1.937(4) 1.965(2)	1.87~2.04
O-Ti-O bond angle	81.2° 90.0°	77.7° 92.6°	81.2°~90.0°

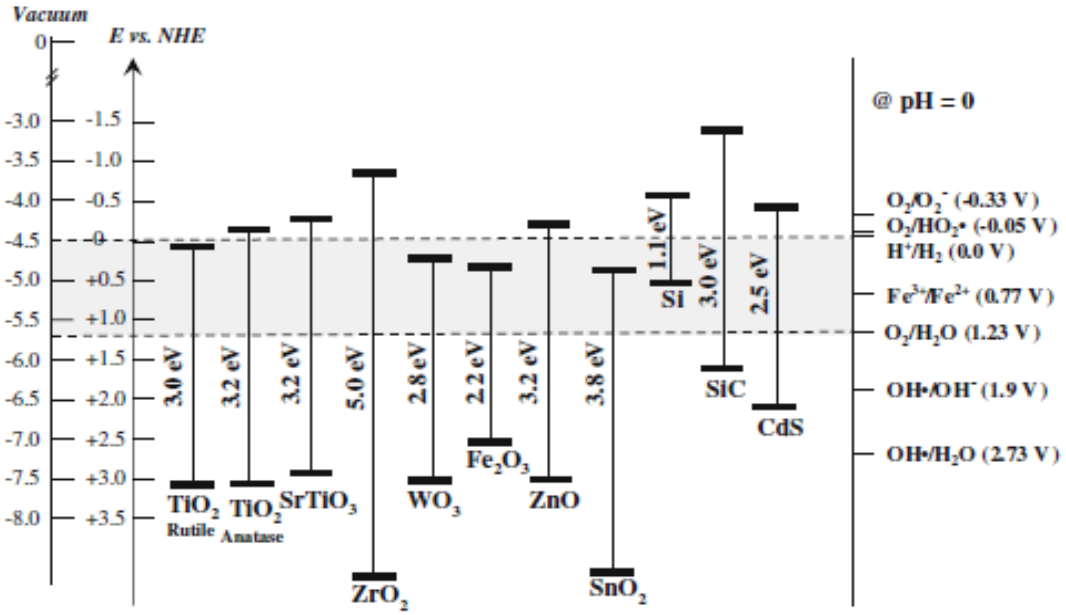

Figure 2.2: Energy level diagram showing valance and conduction band edge positions for various semiconductors at pH 0 referenced against both vacuum and normal hydrogen electrode. Selected redox potentials are presented. [6]

TiO_2 can be prepared in the form of powder, crystals, or thin films. Both powders and films can be built in various particle sizes changing from a few nanometers to several micrometers. The most suitable method for thin film synthesis is sol-gel methods which allow formation of multicomponent structures due to ability of good mixing. Other oxides like silica and dopants can be introduced to the titania thin films derived by this method [7].

Two paths can be followed for the production of TiO_2 with sol-gel method, non-alkoxide and alkoxide. Inorganic salts are as precursors in non-alkoxide routes where metal alkoxides are used in alkoxide routes. Commonly used titanium precursors are titanium(IV) n-butoxide, titanium(IV) ethoxide and titanium(IV) iso-propoxide. Latter in the route TiO_2 sol or gel is formed by hydrolysis and condensation of titanium alkoxides. These reactions are followed by a thermal treatment to remove the organic part and to crystallize titanium dioxide into desired phase [8].

2.1.1. Photocatalysis

Photocatalysis is widely practiced on self-cleaning surfaces, antibacterial surfaces [9], water purification [6], air purification, self-sterilizing surfaces, photocatalytic lithography [10], alcohol reforming [11] and water splitting. One of the most predominant reactions undergoing with the help of titanium dioxide photocatalyst is water splitting. This phenomenon was shown by Fujishima and Honda in 1972 [12]. Their work simply declares that under UV illumination water is decomposed into hydrogen and oxygen on TiO2 photocatalysts. This method still draws attention for solar hydrogen production.

Excitation of titania by a photon having the suitable energy, results formation of an electron at conduction band and a hole in the valance band of the semiconductor. The band gap of anatase is suitable for creation of an electron/hole pair having the capability of reducing and oxidizing an adsorbate, forming a singly oxidized electro donor and a singly reduce electron acceptor, Eqs. (2.1-6) [13].

$$TiO_2 + h\nu \rightarrow TiO_2(e^-, h^+) \quad (2.1)$$

$$TiO_2(h^+) + RX_{ads} \rightarrow TiO_2 + RX_{ads}^{\bullet +} \quad (2.2)$$

$$TiO_2(h^+) + H_2O_{ads} \rightarrow TiO_2 + OH_{ads}^{\bullet} + H^+ \quad (2.3)$$

$$TiO_2(h^+) + OH_{ads}^- \rightarrow TiO_2 + OH_{ads}^{\bullet} \quad (2.4)$$

$$TiO_2(e^-) + O_{2,ads} \rightarrow TiO_2 + O_2^{\bullet -} \quad (2.5)$$

$$TiO_2(e^-) + H_2O_{2,ads} \rightarrow TiO_2 + OH^- + OH_{ads}^{\bullet} \quad (2.6)$$

Processes occurring following to an incident light, electron/hole generation, charge recombination and chemical reactions ran, are illustrated in Figure 2.3.

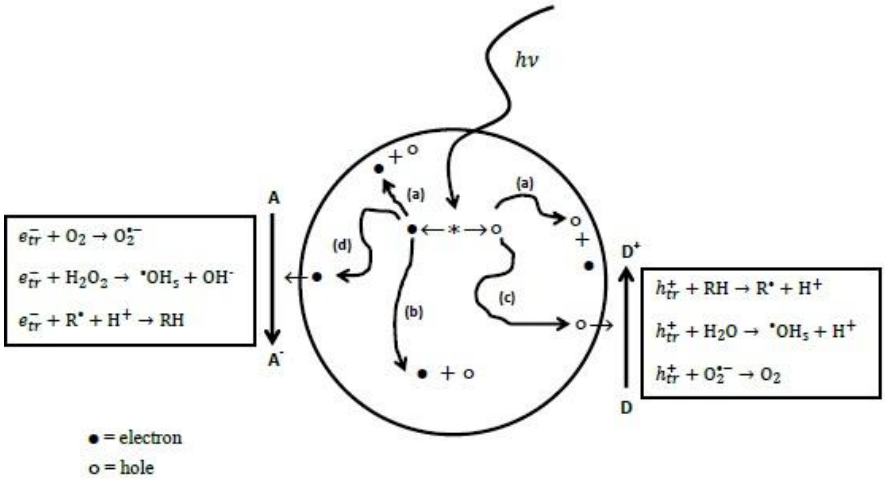

Figure 2.3: Processes occurring on bare TiO2 particle after UV excitation: (a) charge recombination on the surface, (b) charge recombination in the bulk, (c) reaction of photogenerated hole with an electron donor, (d) reaction of photogenerated electron with an electron acceptor. [4]

2.1.1.1. Water Splitting

Water splitting reaction on titanium dioxide was first recorded by Fujishima and Honda in 1972 [12]. In their study it was shown that following to electron/hole pair creation on titanium dioxide, generated electron reacts with water to produce hydrogen.

Simultaneously water is oxidized on valance band of the semiconductor. The reactions occurring on conduction and valance band can be listed as following:

$$TiO_2 + 2h\nu \rightarrow 2e^- + 2h^+ \quad (2.7)$$

$$2h^+ + H_2O \rightarrow 1/2O_2 + 2H^+ \quad (2.8)$$

$$2e^- + 2H^+ \rightarrow H_2 \quad (2.9)$$

$$H_2O + 2h\nu \rightarrow 1/2O_2 + H_2 \quad (2.10)$$

A schematic representation of the reaction is presented in Figure 2.4.

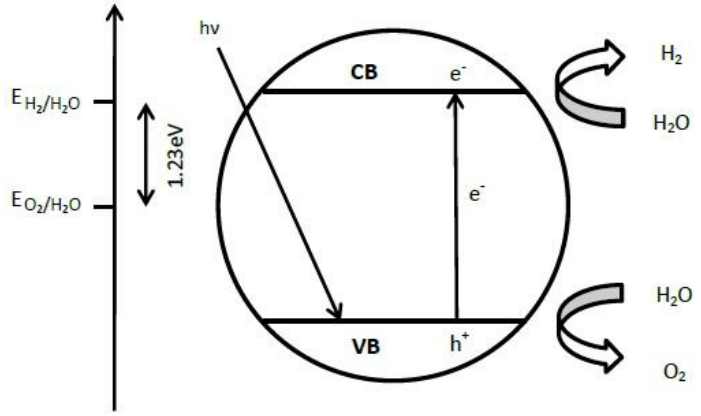

Figure 2.4: Schematic representation of water splitting reactions on TiO_2 particle

In a world of limited energy sources (i.e. fossil fuels) hydrogen energy becomes more and more important every day. One of the main challenges in hydrogen energy is

renewable production of hydrogen. Photocatalytic water splitting is a promising solution to this problem. There are numerous studies found in the literature. [4, 14-22]

2.1.1.2. Quantum Efficiency and Effecting Factors

A performance term of quantum efficiency is defined for photocatalytic reactions. It is the ratio of photons utilized in photocatalytic reaction to photons reaching to photocatalyst. Determination of quantum efficiency is based on the information of how many photons required for the reaction. By this information a product can be related to utilized photon number and that can be divided to total number of photons reaching to catalyst to find the quantum efficiency [23].

Although titanium dioxide is a powerful photocatalyst which runs some very important reactions, there are some problems on photocatalytic efficiency. The problems which limit the photocatalytic activity for most of the reactions taking place on titanium dioxide photocatalyst, especially water splitting reaction can be listed as:

Limited photon harvesting: Photons that can excite TiO_2 photocatalyst, which is UV light represents a small portion of the solar spectrum. Only 4% of solar radiation energy can be collected in UV where this ratio reaches to 50% for visible light. This indicates a limitation in photon harvesting ability of titanium dioxide photocatalysts [20].

Electron hole recombination: Photo-generated electron-hole pairs reported to combine in 1-25μs depending on the reaction medium [24-25]. Fujishima *et al.* records that photocatalytic reactions also occur in time scales of microseconds thus electron hole recombination is a competing phenomenon in photocatalysis [4].

Fast back reaction: For energy increasing reactions, recombination of the energetic species can be observed. For example, photocatalytic water splitting is an energy increasing process, thus back reaction of photocatalytically generated hydrogen and oxygen to produce water occurs easily [20].

2.1.2. Common Solutions of Photocatalytic Efficiency Problems

Here some of very common solutions reported extensively in the literature for efficiency problems encountered in photocatalytic process of titanium dioxide are presented. Noble metal loading, doping, hole scavenging and sensitization are covered.

2.1.2.1. Noble Metal Loading

Noble metals have Fermi levels lower than titanium dioxide which makes them to attract the excited electron on the conduction band of the semiconductor and act as an electron trap. This provides the charge recombination. Pt, Pd, Ag and Au are shown to be effective loadings for increasing quantum efficiency of titanium dioxide [26].

Lu *et al* studied effect of different noble metal loading on photocatalytic hydrogen generation over eosin sensitized titanium dioxide. Pt, Pb, Ru and Rh were used as different noble metals in the study and results show that noble metal loading shows considerable increase in hydrogen generation under visible light having wavelength larger than 420nm. Positive effect observed for these four noble metals can be listed as Rh>Ru>Pb>Pt. Hydrogen evaluation also increased for increasing ratio of noble metal to titania up to 10%. Highest quantum efficiency recorded in the study is 10.27% [27].

2.1.2.2. Doping

Metal and non-metal doping is another technique utilized in TiO2 semiconductors. Creation of sinks for photogenerated electrons or holes is the main idea for this procedure. But the impurity energy levels formed in the band gap of titania also results an increase in the visible light harvesting ability [20].

Metal dopants such as Fe, Mo, Os, Re, V, Cu, Co and Ni are studied extensively [28-29]. Ni *et al.* reported that an optimum concentration for metal doping is present over which the photocatalytic activity decreases as a result of increasing charge recombination. It is also reported that Cu and Fe ions enhance the photocatalytic activity by introducing impurity energy level near to both conduction and valance bands of titania [20].

Doping anions such as N, F, C and S is rather new technique in the literature. Non-metal dopants also reported to increase the photon harvesting as well as preventing the charge recombination [20].

2.1.2.3. Addition of Hole Scavengers

In order to prevent electron hole recombination, a sacrificial agent of hole scavenger (or electron donor) can be introduced to the system. These species irreversibly react with the photogenerated holes on the valance band of the semiconductor which is illustrated in Figure 2.5. This results an increase electron hole separation thus quantum efficiency [20]. As a result of the irreversible interaction, these chemicals are called sacrificial agents. Depletion occurs as the reactions proceeds and renewal is needed.

Nada *et al*. studied the effects of different hole scavengers on the photocatalytic efficiency of water splitting reactions. For various hydrocarbons, increase in photocatalytic efficiency is recorded to be highest for EDTA followed by methanol, ethanol and lactic acid respectively. It was also recorded that decomposition of those hydrocarbons had effects on hydrogen production since hydrogen is a product for their decomposition [30].

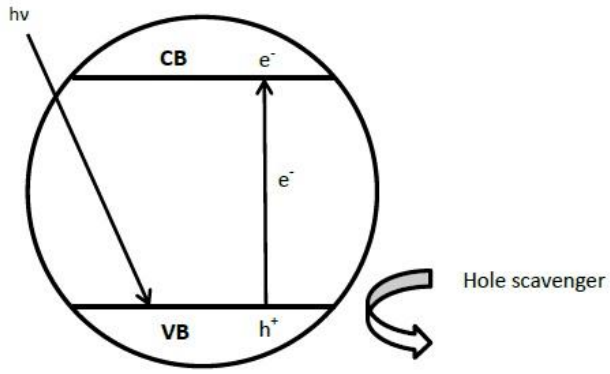

Figure 2.5: Schematic representation of hole scavenging on photocatalyst.

2.1.2.4. Sensitization

Sensitization is making the photocatalyst sensible to less energetic light compared to its band gap. This process moves the adsorption threshold of the catalyst to higher wavelength (i.e. to the visible spectrum). This is called red shift and it provides the excitation of the photocatalyst with less energetic photons.

Sensitization processes are commonly conducted by introduction of a sensitizer dye or another semiconductor to the reaction environment. Sensitizing material should be selected in a manner that, the added material should be exited with a less energetic photon than titanium dioxide and generated electron should be at an energy level higher than titanium dioxide. Process is illustrated in Figure 2.6.

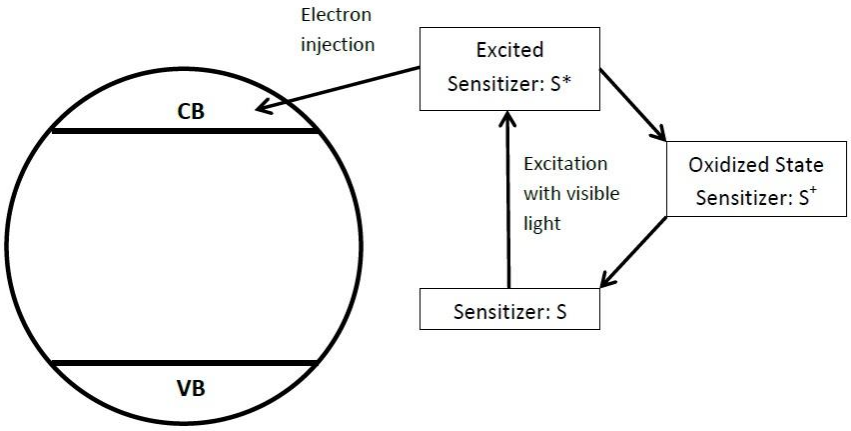

Figure 2.6: Schematic representation of sensitization.

Gratzel *et al.* showed that dye-sensitization can increase the photon harvesting ability of the titanium dioxide. In this work a monolayer of trimeric ruthenium complex on titanium dioxide thin film of 10µm. TiO_2 film which was initially transparent, colorized to deep brownish-red. The absorption threshold of thin film shifted to 750nm where 100% light harvesting efficiency was recorded for whole the visible region below 550nm. Overall light to electric yield is recorded between 7-12% for the solar cell utilizing these films [31].

Kaneko *et al.* studied dye sensitization of titanium dioxide in the presence of hole scavenger for photocatalytic water splitting. $Ru(bpy)_3^{2+}$, $Ru(bpym)_3^{2+}$ and porphines were studied as sensitizers for platinized titania. $Ru(bpym)_3^{2+}$ found to be as efficient as known sensitizer of $Ru(bpy)_3^{2+}$ in terms of visible light hydrogen production. EDTA was used as hole scavenger in the study. A comparison with different hole scavengers, including ascorbic acid, was also conducted. EDTA found out to be highest active hole scavenger for photocatalytic water splitting [15].

2.1.3. SiO_2/TiO_2 Thin Films

Thin film is an important form of titanium dioxide for photocatalytic applications. Transparent films having thicknesses comparable to wavelength of illumination source, achieves perfect illumination of the catalyst surfaces.

Dip-coating is the mostly used coating technique. Thickness of the films can be controlled easily and multilayer formation can be achieved by this method which dip-coating advantageous over other sol-gel coating techniques, such as spin coating and spray coating. The process involves the formation of a film through successive steps of immersion of substrate into the dip-coating solution and withdrawal of the substrate form the solution at a constant rate. After the substrate is removed from the solution, solvent is evaporated. Viscous drag, gravitational forces, surface tension of the curved meniscus affects the thickness of the film that is formed. Also, sticking probability of the precursor and aggregation plays role in the thickness [32]. Coating process is finished with thermal treatment stage. Typically, sol−gel-derived precipitates are amorphous and in order to introduce crystallization controlled heat treatment is applied. To remove the entrapped solvent, and any organic remaining, thin films are dried and calcined at appropriate temperatures [8].

Low surface area of pure titanium dioxide materials is another factor limiting the photocatalyst performance. Preparation of binary catalyst of titanium dioxide with relatively higher surface area materials such as silica can be a solution for this problem. Bard *et al.* reported higher photocatalytic activities for silica/titania sol-gel derived photocatalyst with respect to pure titania photocatalyst. The work also showed that there is an ideal ratio for silica/titania which is reported to be 30/70 (wt/wt) in the study [33].

For further increase in the surface area organic materials, such as PEG could be utilized as molecular templates. These templates mixed to synthesis mixtures are burnt down and removed in the calcination step of catalyst preparation. Yu *et al* studied effect of PEG addition for titanium dioxide thin films prepared by sol-gel method. They observe

an increase in photocatalytic activity to a certain extend with increasing PEG addition. But over a certain value they observe a decrease in the reaction rate. Study explains that, the decrease in the reaction rate is due to increasing scattering with increasing porosity. More the light scatters, less energy is transmitted to the active sites they conclude [34].

2.2. Ascorbic Acid

Ascorbic acid is one of the most powerful antioxidant in biological systems. Antioxidants are substances that can delay, inhibit or prevent the oxidation by scavenging free radicals. Effectiveness of the antioxidants is measured with the normalization to ascorbic acid [35]. Thus ascorbic acid can be utilized as hole scavenger in the photocatalytic reaction. There are also several studies also suggest that ascorbic acid can also be used as sensitizer for photocatalyst [36-37].

Rajh *et al* conduct a study to observe the effect of ascorbic acid adsorption on titanium dioxide and they found that the adsorption of ascorbic acid on titanium dioxide nanoparticles leads 1.6eV of red shift in band gap. They also stated that the electron donating site in the electron transfer mechanism found to be ascorbate modifier bound to the surface where the accepting site is conduction band of titanium dioxide [36].

Liao *et al* studied effect of ascorbic acid presence on photocatalytic activity of titanium dioxide in powder form by similar methyl orange decomposition tests. They observed red shift of absorption threshold of titanium dioxide in the presence of ascorbic acid. The paper also suggested a mechanism for the interactions between ascorbic acid and titania which enhance the activity. It is reported that binding of ascorbic acid to titanium dioxide as result of the interaction with the hole created there is present [37].

2.3. EDTA

Organic carbons are widely used as hole scavengers as they are oxidized by the valance band of semiconductor. EDTA is one of the most commonly used hole scavenger in this context [20].

EDTA is used as a reference to compare the effectiveness of chemical additive to titanium dioxide photocatalyst. Qu *et al.* studied rhodamine B (RB) degradation on titania surfaces and the effect of several chemical additives including EDTA. In addition to those, they also proposed a degradation mechanism for RB [38].

In the literature, there are studies comparing the photocatalytic enhancement created by EDTA and ascorbic acid [27]. Kothari *et al.* compares effect of ascorbic acid and EDTA on photocatalytic reduction of malachite green on cadmium sulfide catalyst [39].

2.4. Methyl orange degradation

Photocatalytic degradation of azo dyes is studied extensively for water purification [6]. [37, 40] Degradation of these dyes is also utilized as probe reaction to measure the photocatalytic activity of the catalyst synthesized and modified [41].

Rate of methyl orange degradation can be measured with correlating it with the decolorization of the solution. Ou *et al.* used UV-Vis spectrometer data for methyl orange solution at 464nm, to measure the concentration of methyl orange. The calibration for the spectrophotometer used in the study, error is reported to be less than 5% [37].

Konstantinou *et al* reported that most of azo dyes including methyl orange (acid orange 52) strongly adsorbed on titania for pHs lower than 6, due to electrostatic attraction between dye and positively charged TiO_2. It is also reported that for pHs greater than 6.8, charge of titania changes and due to Coulombic repulsion between dye and titania,

dyes are scarcely adsorbed. This results a decrease in the photocatalytic activity for degradation of dyes in the pH range 7-11 [42].

CHAPTER 3

EXPERIMENTAL

3.1. Catalyst Preparation

Investigation of the effect of PEG addition on catalyst surface area and photocatalytic reaction rates were in the scope of this study. In order to investigate these effects catalyst with different specifications were prepared. Sol-gel procedure was used to synthesize the catalysts and that step is followed by dip coating or powder preparation to obtain the desired catalyst.

3.1.1. Sol-Gel Preparation

Catalyst samples used in this study was synthesized by sol-gel method. The recipe used for this method is based on the study performed by Beril Korkmaz Erdural [43]. Titanium tetraisopropoxide (TTIP, Aldrich, extra pure grade, CAS: 7647-01-0) was used as precursor for synthesis. On the synthesis, first 200mL UP grade (with 16.8MΩ conductivity) water added into 500mL glass balloon. Later 1mL of acetic acid added was followed by dropwise addition of 5mL TTIP to the mixture. After the addition of TTIP, 700uL nitric acid is added to solution. The solution placed in a water bath kept at 80°C for 30 minutes for gelation. The colloidal solution was removed from the water bath and kept in room temperature for 2 hours afterwards for cooling. Cooling of the solution was followed by further dropwise addition of 6.4mL LUDOX® solution (SM-30, Aldrich) as a silica source. Silica added colloidal solution was kept in the dark at

room temperature overnight for aging. 2 hours prior to the usage, specified amount of PEG (MW=6000, Acros Organics) dissolved in 100mL UP grade water added and to colloidal solution. Constant stirring was present throughout the whole procedure.

3.1.2. Film preparation

Thin films were coated on glass surfaces by dip coating technique. Glass specimens used for coating were microscope slides with dimensions of 76mmx26mmx2mm. Glass substrates first rinsed with UP grade pure water and technical grade ethanol and immersed in 1M KOH solution overnight. The slides were washed with UP grade pure water and technical grade ethanol. Lastly, washed slides were dried in 120°C oven for 10 minutes prior to coating. Dried slides were mounted on dip coating apparatus (Figure 3.1) and 5 successive layers of thin film were coated on each slide. Each layer of thin film was coated as a result of a single dipping of glass substrate into colloidal solution and pulling out of solution. Dipping rate of 20 mm/s and pulling rate of 2 mm/s were used to form a film thickness of approximately 500nm-750nm [34]. Between each dipping and pulling stage slides were kept in the colloidal solution for 1 minute.

Between successive coatings, the slides were dried at 120°C in a preheated oven. Subsequent to the coating steps, the slides were placed in 500°C preheated tubular furnace (Protherm 1000W, PTF 12/50/250) with steady air flow for and calcined for 15 minutes.

3.1.3. Powder Preparation

The colloidal solution prepared was poured in ceramic plates, kept in oven at 120°C for 3 days to achieve drying. After that, dried gel was transferred in a quartz cuvette and

placed in a preheated tubular furnace at 500°C under air flow. The gel was calcined in the furnace for 3 hours and the solid clumps were reduced to powder by mortar.

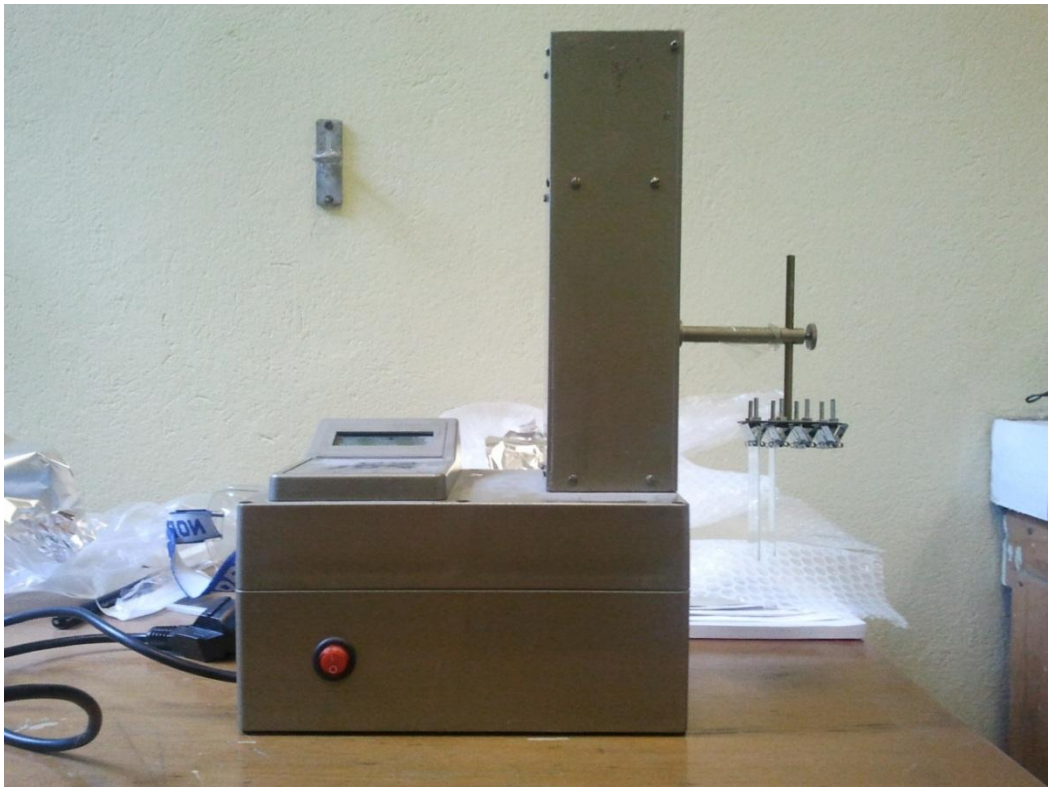

Figure 3.1: Dip coating apparatus.

3.2. Characterization and Activity Measurements

Catalysts synthesized by sol-gel methods were first investigated in terms of surface area with a methylene blue adsorption method [44]. Later the photocatalytic activities of the catalysts are measured in artificial sun light simulator and 254nm UV light chamber.

3.2.1. Methylene Blue Surface Area Measurement

The surface area measurements for thin film samples were performed by a previously developed method by Burcu Koç. [44] Thin film coated substrates having the same dimensions (20 x 26 mm) were immersed into separate methylene blue solutions having different concentrations (20mL of 1, 2, 3 and 4 ppm) for adsorption. The saturation was ensured by extending adsorption period until the constant concentration of solution was read on absorbance at 661nm wavelength which is monitored by UV-Vis spectrophotometer. Then the films are removed and concentrations of remaining MB solutions measured by spectrometer were recorded. The adsorption data was fit into a Langmuir isotherm to determine the relative surface area (surface area of thin film per unit area of substrate).

3.2.2. Methyl Orange Degradation Experiments

10ppm methyl orange solution was prepared by mixing 100mL UP grade pure water with 25mL 50ppm methyl orange stack solution in 400mL beaker. Variable amounts of ascorbic acid were added to the solution and pH of the solution was adjusted to 4, 7, and 10 by adding proper amount of sodium carbonate. The activity of powder catalyst samples was determined by methyl orange degradation test by adding powder catalyst directly to methyl orange solution and maintaining the suspended form by mixing. The activity of thin film samples were tested by immersing the samples in the solution at 1.5cm depth from the surface and irradiating from the top while mixing the solution by magnetic stirrer. The methyl orange solution volume in the beaker was kept constant throughout the experiment by adding sufficient amount of UP level pure water. Beaker was placed in a sun simulator (Atlas SUNTEST CPS+) and irradiated with a power density of 300W/m2 in 300-800nm wavelength. Liquid samples from the solution were collected at every 15 minutes and immediately analyzed with UV-Vis Spectrophotometer, working in scanning mode between 200nm to 800nm.

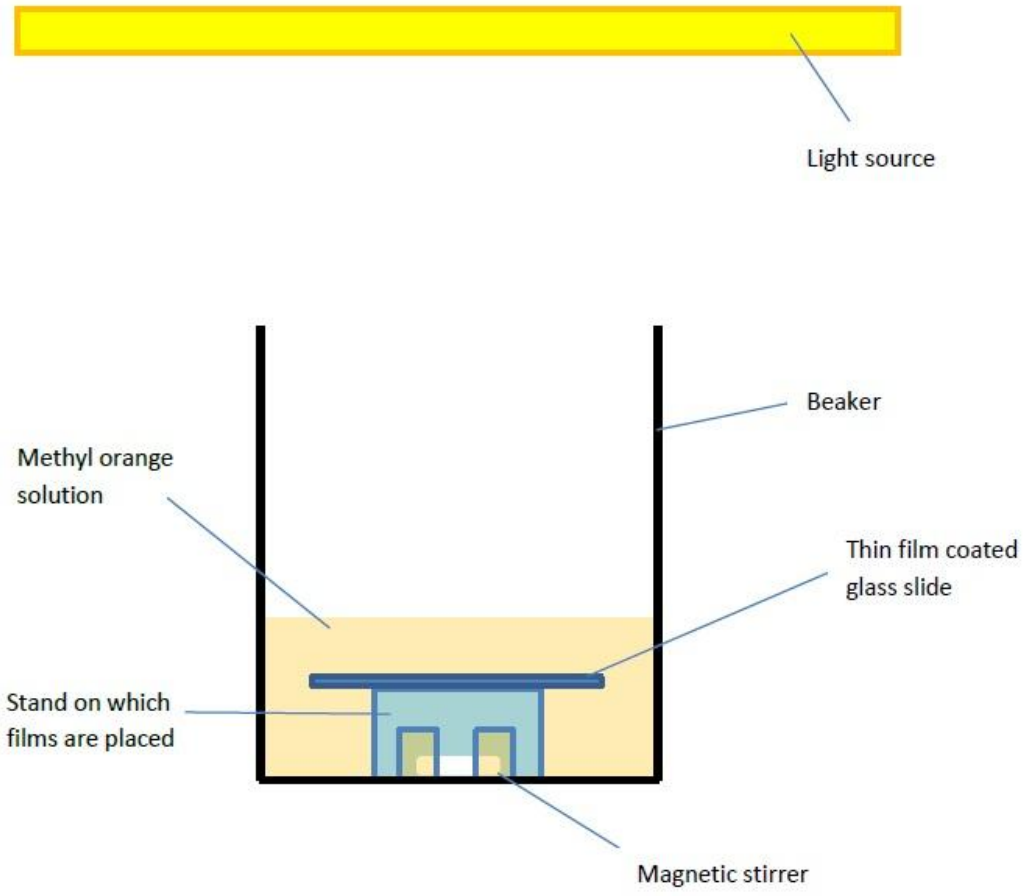

Figure 3.2: Experimental setup placed in sun simulator in which methyl orange degradation experiments run.

3.2.3. Water Splitting Tests

A quartz volumetric flask having 7mL volume was used as a reactor. The reactor tube is placed in the center of cylindrical irradiation chamber having 100mm inner diameter, 285mm height and 3 of 12W Hg lamps located at each corner. Each lamp can be operated singly.

Desired amounts of AA and EDTA were dissolved in UP grade pure water and mixed with catalyst sample before the experiment. Then the neck of the flask is connected to open end u-tube trap which is sealed by 10cm column of UP grade water. The reaction is initiated by switching on the UV lamps and the volume of evolved gas was measured by recording the height of water trap in u-tube column and temperature. The volume and the temperature data with respect to time were converted into molar rates by ideal gas assumption.

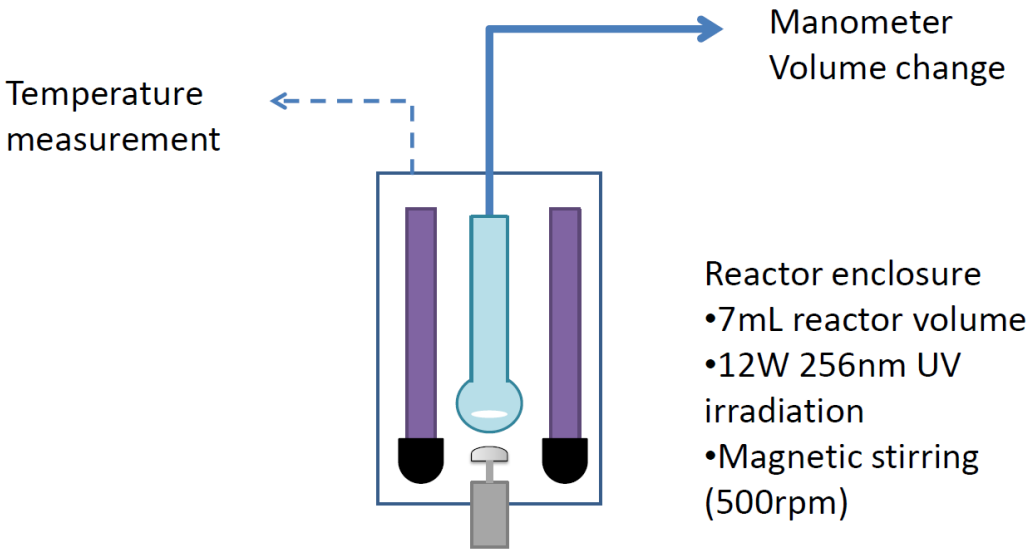

Figure 3.3: Experimental setup used for experiments conducted under UV light.

3.2.4. Ascorbic Acid Photoadsorption Experiments

Adsorption of ascorbic acid on catalyst thin films was also investigated. Prepared thin films were dipped in a constant concentration ascorbic acid solution. The solutions, with the films inside, were placed in sun simulator device. Adsorption on the thin film surfaces was investigated with UV-Vis spectrophotometer. Prior to investigation films were removed from the solution and dried. Then the absorbance spectra of the films were obtained by spectrophotometer. Device is operated in the scanning mode in the range of 200nm to 800nm wavelength. Change in the peak structures, positions and magnitudes were analyzed to extract information about ascorbic presence on the films. The procedure was repeated at the end of each 1 hour illumination in solar simulator for 3 hours in order to obtain the transient data for methyl orange adsorption on the film.

CHAPTER 4

RESULTS AND DISCUSSION

Relatively low surface area of TiO2 thin films is a limiting factor for photocatalytic activity. To increase the surface area of thin film thin film photocatalysts PEG is used as a template for pores during the synthesis. The effect of PEG addition on film surface area and photocatalytic activity is studied in the first part.

Sensitization potential of ascorbic acid is the main focus of this study. In the second part, the effect of ascorbic acid addition on photocatalytic activity of titanium dioxide is investigated. Photocatalytic degradation of methyl orange under different reaction mediums are applied for this aim.

Ascorbic acid is an important antioxidant in biological systems. Antioxidants are hole scavenging agents. In the final part, effect of ascorbic acid on photocatalytic activity of thin films is compared with a well-known hole scavenger sacrificial agent, EDTA solution.

4.1. Thin Film Coating

Sol-gels recipes with 10g, 18g, 27g and 40g PEG addition were prepared according to the synthesis method described in the experimental part. Thin film samples were obtained from the colloidal solutions, on microscope slides by 5 successive coating-drying steps. The surface areas of coated films were measured with methylene blue

adsorption method described in the experimental part. Methylene blue concentrations were measured by UV-Vis spectrophotometer.

4.1.1. The Surface Area of Thin Films

Absorption readings for different compositions of methylene blue solutions were interpreted to relative surface area of films with respect to slide area. Figure 4.1 illustrates the change in the relative surface area with change in the addition of PEG.

Relative surfaces areas were calculated by using the following equation:

$$S = \frac{L \times A_{MB} \times x_m}{N} \tag{4.1}$$

where

S : Relative surface area

x_m : Monolayer adsorption capacity

L: Avogadro number

A_{MB} : Area covered by a single adsorbed methylene blue molecule

N : Molecular weight of methylene blue

Monolayer adsorption capacity is found by fitting the experimental values to a Langmuir equation of;

$$\frac{C_E}{x/m} = \frac{1}{kx_m} + \frac{C_E}{x_m} \tag{4.2}$$

where

C_E : Equilibrium concentration of remaining methylene blue in the solution

x/m : Quantity of methylene blue adsorbed on unit area of adsorbent

k : Langmuir constant

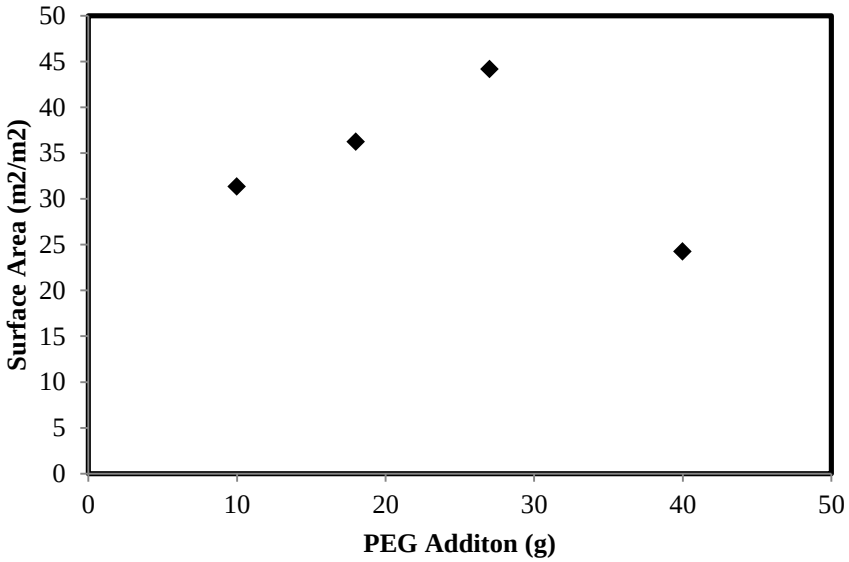

Figure 4.1: Surface Area measurement for glass slides coated with titania sol-gel containing 10g, 18g, 27g and 40g of PEG.

Results show that the relative surface area of thin film samples increases with increasing PEG addition to certain extend. This is an expected result since PEG was used as a molecular template for enhancing the porosity and surface area of the samples. Thus, porosity and surface area in result increased with increasing PEG content. A peak value was observed for the film coated with 27g PEG containing sol-gel. And further increase in PEG content caused a decrease on the surface area of the films. Increasing pore volume made the solid network of metal oxide thinner and weaker. Over a threshold value solid network would not be able to support itself anymore thus the structure collapses. This may be a result for sharp decrease in the surface area for increasing PEG content.

4.1.2. Methylene Blue Activity Test

Effect of surface area of the catalyst on the photocatalytic efficiency was tasted with the probe reaction of methylene blue degradation test. The thin film samples were first saturated with methylene blue for surface area characterization and then used to test methylene blue degradation tests. Decolorization of methylene blue was examined to measure the extent of degradation and the effect of PEG addition or in other words, effect of surface area on photocatalytic activity of the thin films. The degradation tests were performed under artificial solar irradiation and UV-Vis absorbance of the films were recorded as a function of exposure time to follow reaction time course. The initial concentration of methylene blue and the samples taken 15 min interval were determined by the absorbance of methylene blue at 661nm by UV-Vis spectrometer. Figure 4.2 illustrates concentration change of methylene blue with time.

Kinetic analysis of the degradation reaction was performed by assuming pseudo first order reaction mechanism [40]. Rate constants were calculated by fitting the experimental data to an exponential function in order to validate first order rate expression. (Equation 4.3)

$$-\ln\left(\frac{C}{C_0}\right) = kt \tag{4.3}$$

Linear regression method was applied to each processed experimental data shown in Figure 4.3. R^2 values for regressions were generally observed to be over 0.9. That was interpreted as the assumption to be valid.

Rate constants found as the slopes of the lines fitted to the curves are presented in Figure 4.4. Regarding Figure 4.1 and Figure 4.4, results show correspondence with the surface area measurements. It can be stated that the photocatalytic activity increased with increasing surface area. But over a certain value, activity decreased. Yu *et al.*

explains that the decrease with increasing PEG addition is due to decrease in the transmitted energy to the catalyst due to increasing scattering. [34] But it can be also explained as the decrease in the surface area.

There is also a decrease in the rate constants with increasing surface concentration of MB for each film having the same PEG content. This situation is best observed in 27g PEG containing films (PEG27) in Figure 4.4. This decrease in rate constants indicates that the adsorbed amount of MB over the film surface also shows a resistance for the reaction.

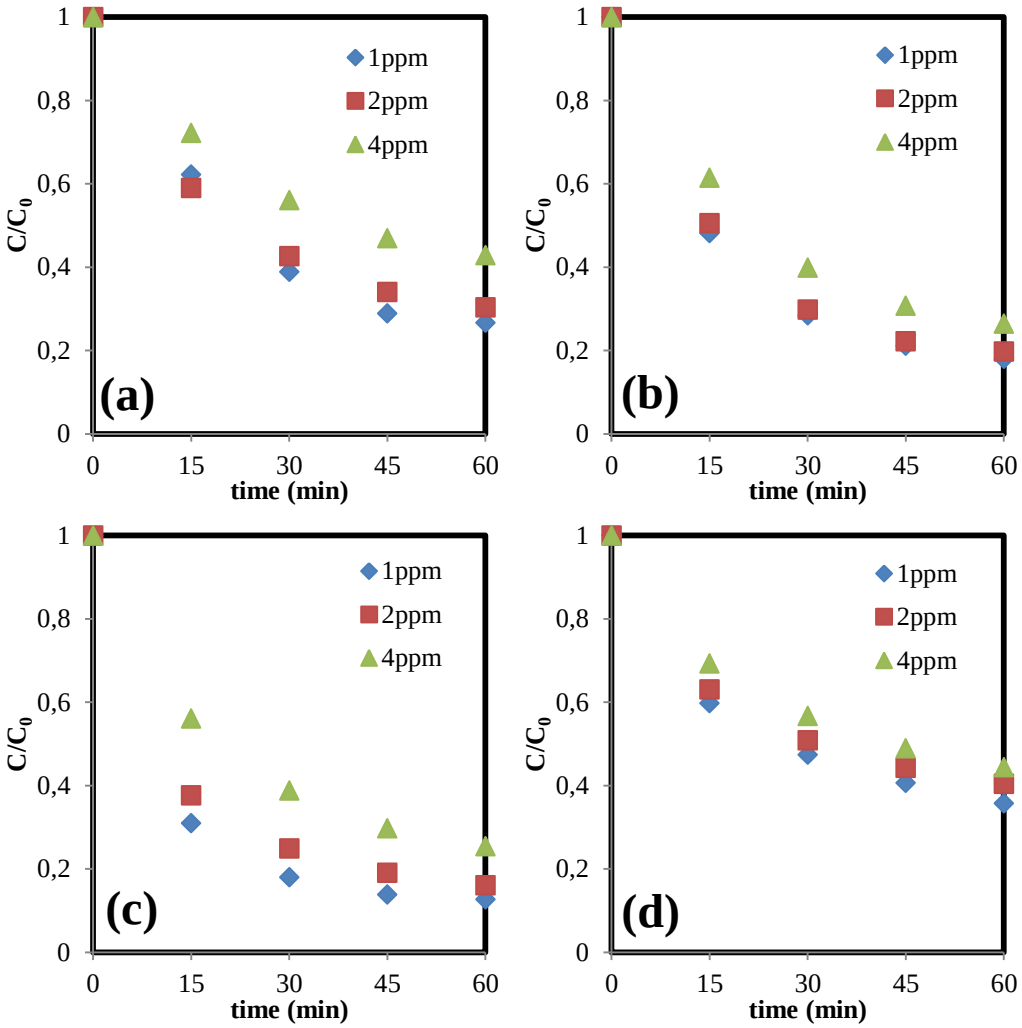

Figure 4.2: Change of methylene blue concentration with time in methylene blue degradation experiment for (a)10g, (b)18g, (c)27g and (d)40g PEG addition.

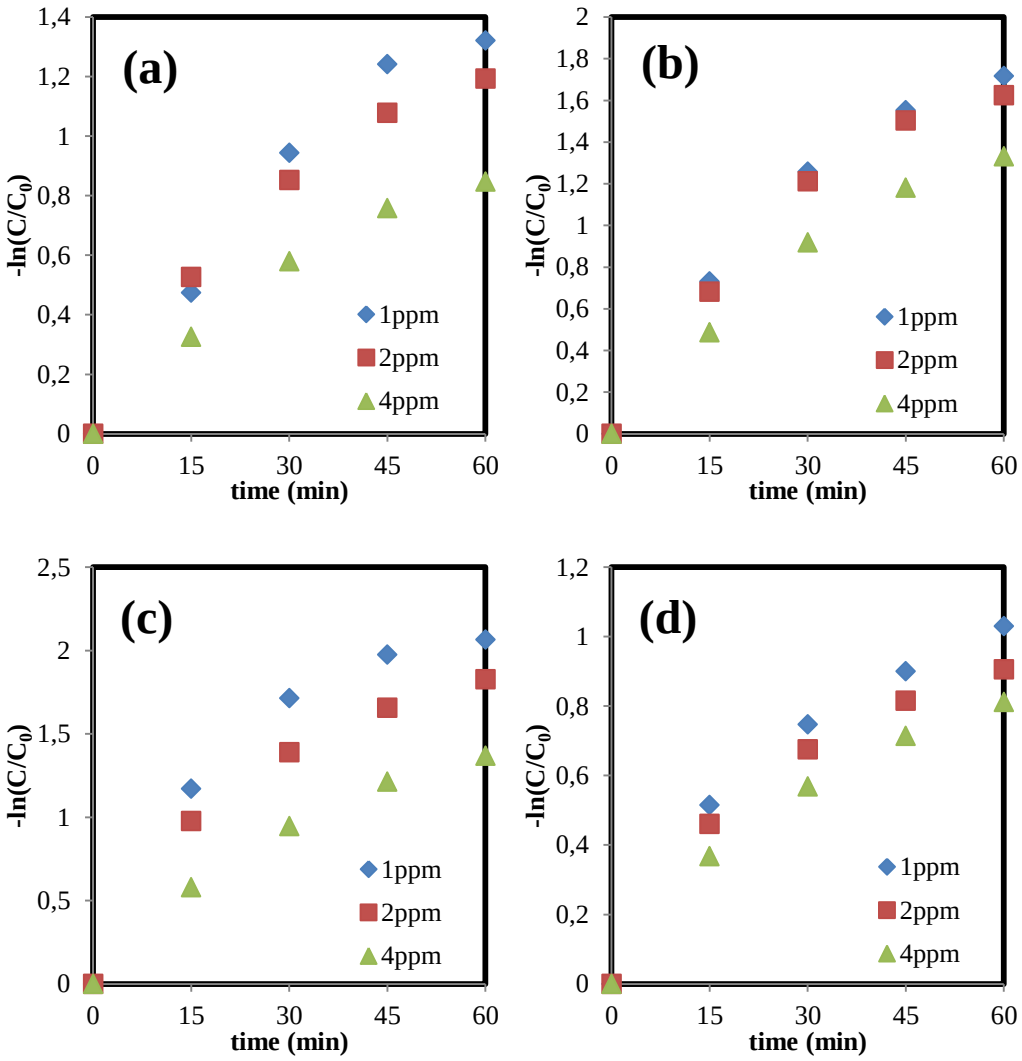

Figure 4.3: Pseudo first order reaction behavior of methylene blue degradation experiment for (a)10g, (b)18g, (c)27g and (d)40g PEG addition.

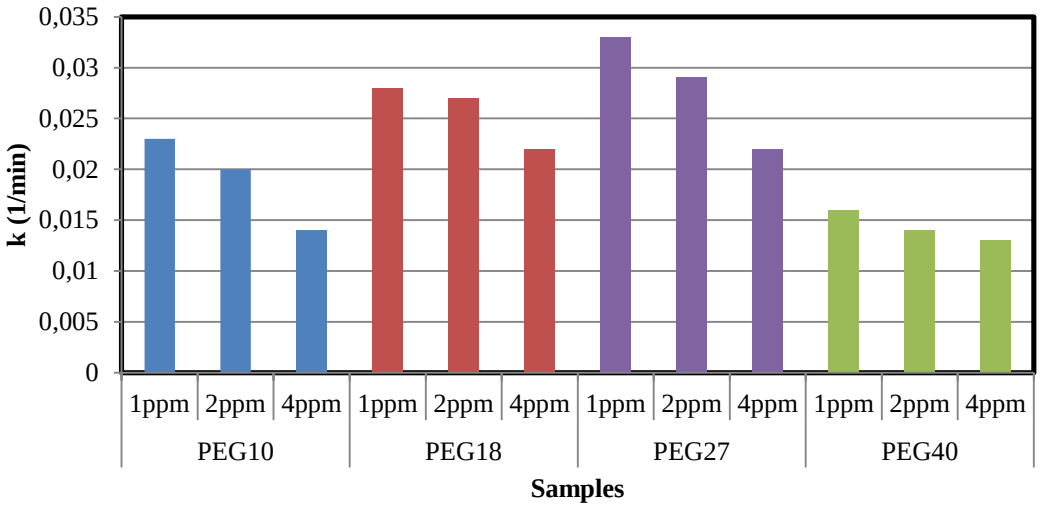

Figure 4.4: Rate constants calculated for (PEG10) 10g, (PEG18) 18g, (PEG27) 27g and (PEG40) 40g PEG addition.

4.1.3. Ascorbic Acid Adsorption Test

In order to measure the effect of adsorption on sensitization ability of ascorbic acid, the adsorption experiments were performed. First, the thin film samples were immersed in the ascorbic acid solutions having various concentrations in the dark and the adsorption was followed by the UV-Vis spectroscopy of the samples. But no significant absorption was observed. When the experiments were repeated under the artificial solar irradiation, change in the UV-Vis absorption spectra was observed. This was interpreted as photo-adsorption and change in the spectra with respect to time were investigated. Results for 10g, 18g, 27g and 40g PEG added films are presented in Figures 4.5-8. respectively.

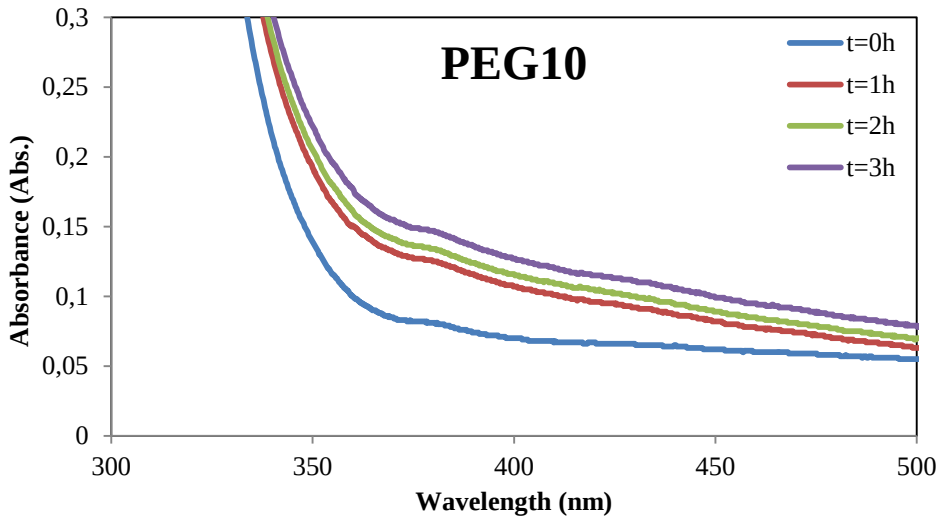

Figure 4.5: UV-Vis spectra show the change in the absorbance of thin film derived from 10g PEG added sol-gel kept in ascorbic acid solution with respect to time.

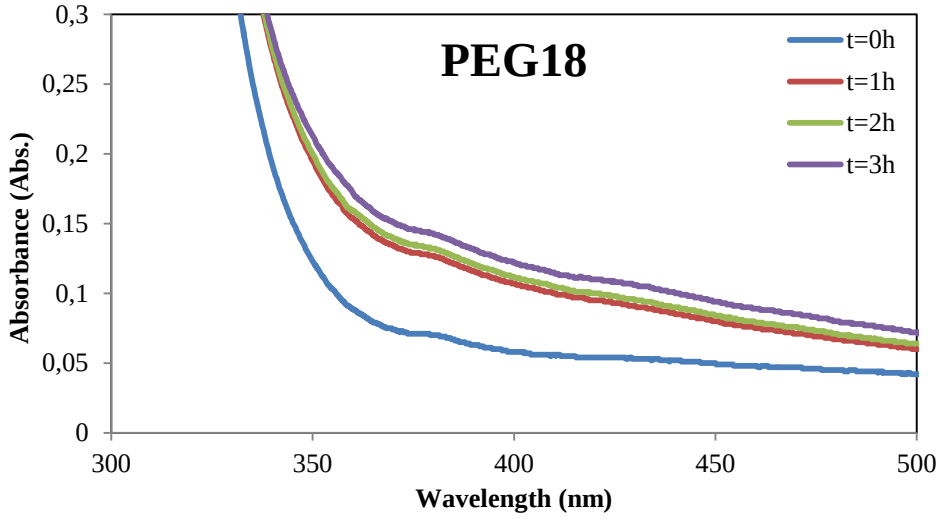

Figure 4.6: UV-Vis spectra show the change in the absorbance of thin film derived from 18g PEG added sol-gel kept in ascorbic acid solution with respect to time.

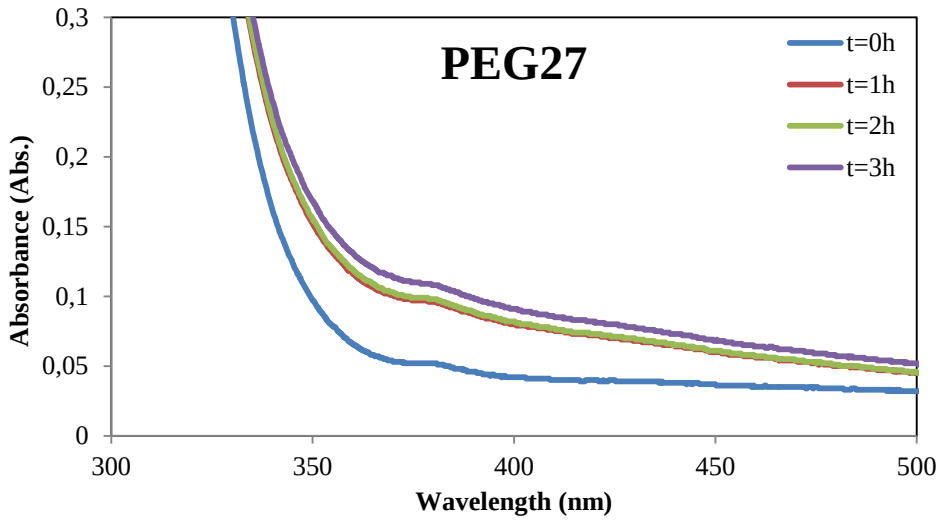

Figure 4.7: UV-Vis spectra show the change in the absorbance of thin film derived from 27g PEG added sol-gel kept in ascorbic acid solution with respect to time.

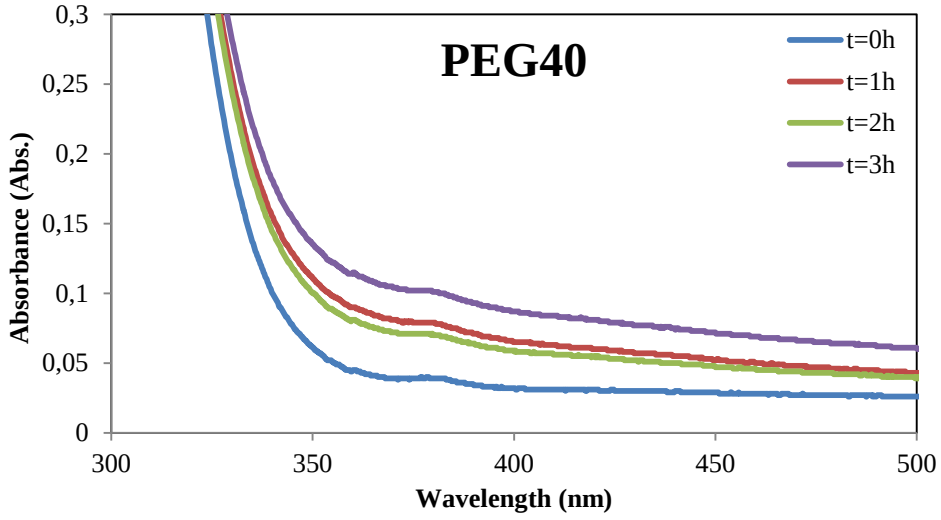

Figure 4.8: UV-Vis spectra show the change in the absorbance of thin film derived from 10g PEG added sol-gel kept in ascorbic acid solution with respect to time.

These results indicate the faster photo adsorption of ascorbic acid to the samples with higher surface area. The rate of adsorption for film samples were calculated by linear regression of time change of absorption data recorded for 380nm. Results are presented in Table 4.1. After initial hour of adsorption, change is minimum for 27g PEG added sample. It is followed by 18 PEG containing samples. And change is maximum for 10 and 40 g PEG containing samples. This shows that for higher porosity samples adsorption yields to saturation in shorter time periods.

Table 4.1: Rate of methyl orange adsorption after 1 hour on 10g (PEG10), 18g (PEG18), 27g (PEG27) and 40g (PEG40) PEG containing film samples

Sample	Rate (change in abs/h)
PEG10	0.011
PEG18	0.008
PEG27	0.006
PEG40	0.011

4.2. Effect of Ascorbic Acid on Photocatalytic Activity

The viability of ascorbic acid sensitization was intended to test with a probe reaction. The methylene blue degradation tests were found not suitable for this purpose because of fast decolorization of methylene blue in the presence of ascorbic acid. Ascorbic acid is highly reactive with methylene blue and decolorize 100ppm methylene blue solution within few minutes. However, the preliminary experiments performed with methyl orange showed no significant interaction with ascorbic acid. Therefore, the sensitization

effect of ascorbic acid was characterized by selecting the photocatalytic degradation of methyl orange as probe reaction.

4.2.1. Methyl Orange Degradation and Effect of Ascorbic Acid Sensitization

Activities were measured with methyl orange degradation experiments. Concentration of methyl orange was determined by using UV-Vis spectrophotometer. Methyl orange solutions showed an absorbance peak at 499nm in the range of 200-800nm. The spectrometer was calibrated for methyl orange concentration at this wavelength (Figure B.1).

Methyl orange degradation tests were conducted as described in the experimental section. The concentration-time data were analyzed by assuming first order kinetics [42] and the absorbance values at 499nm were directly related with concentration as;

$$\frac{C}{C_0} = \frac{A}{A_0} \tag{4.4}$$

The experiments performed with both powder and thin film forms of the samples. The effect of ascorbic acid concentration and the blank experiments without catalyst and in-dark were analyzed by linear regression of $-\ln(A/A_0)$ vs. time data. The experimental results are compared in Figure 4.9.

The blank experiment in-dark yielded no significant reaction in the absence of catalyst. However, the methyl orange degradation takes place in the presence of light which can be attributed to photodecomposition of methyl orange in the presence of ascorbic acid. It was also observed that in the presence of commercial titanium dioxide powder, degradation also took place in the presence of light. This is interpreted as photocatalytic degradation of methyl orange. And in the presence of both, ascorbic acid, film catalyst and light, decomposition of methyl orange was observed again. For the same amount of

ascorbic acid presence, in the presence of film catalyst decomposition of methyl orange took nearly two times faster, in the presence of light.

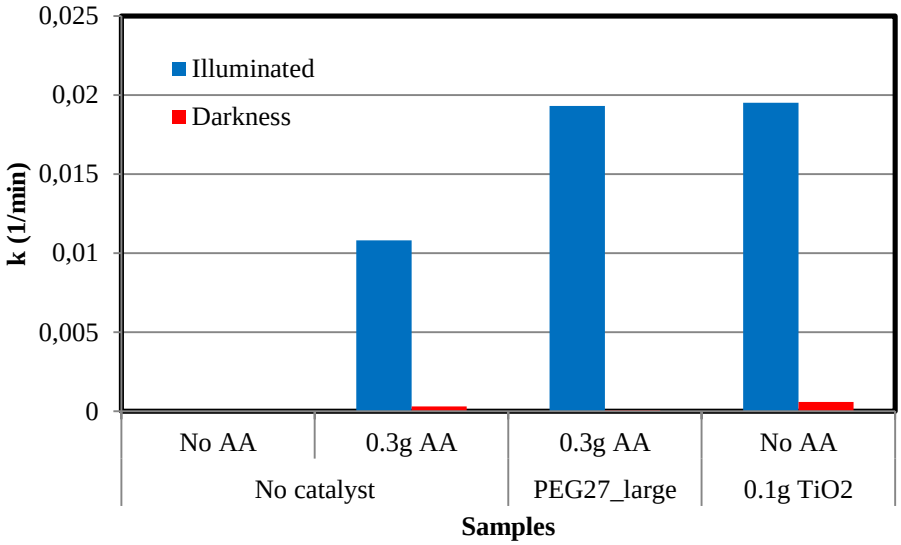

Figure 4.9: Comparison of rate constants for different catalysts with and without ascorbic acid in illuminated and dark chambers.

The effect of ascorbic acid concentration in the presence of catalyst samples synthesized with 18g and 27g of PEG were also studied under 300W/m2 300-800nm irradiation. The change in methyl orange concentration with respect to time and the results of the data analysis by assuming first order degradation kinetics are shown in Figure 4.10, Figure 4.11 and Figure 4.12.

.

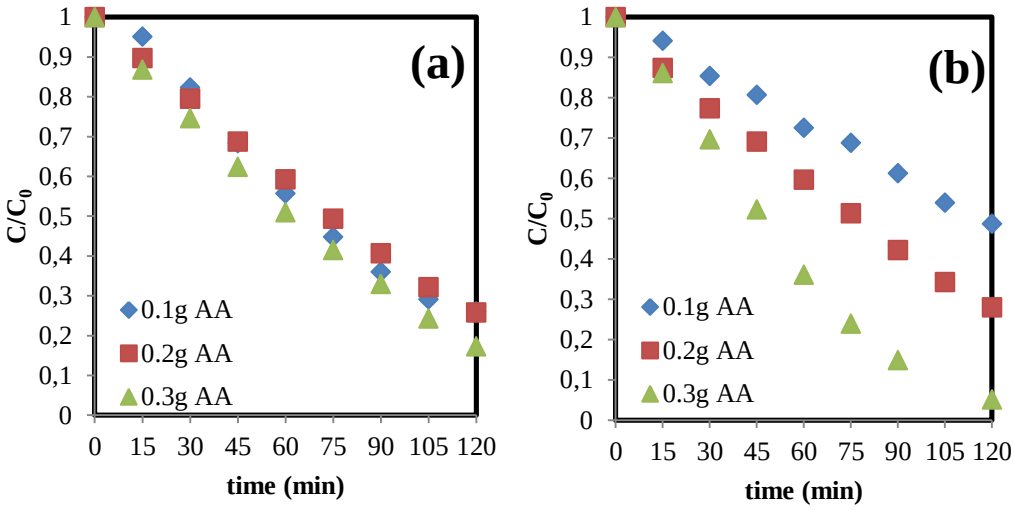

Figure 4.10: Change of concentration of methyl orange in photocatalytic degradation experiment for (a) 18g and (b) 27g PEG containing samples with 0.1g, 0.2g and 0.3g Ascorbic Acid addition.

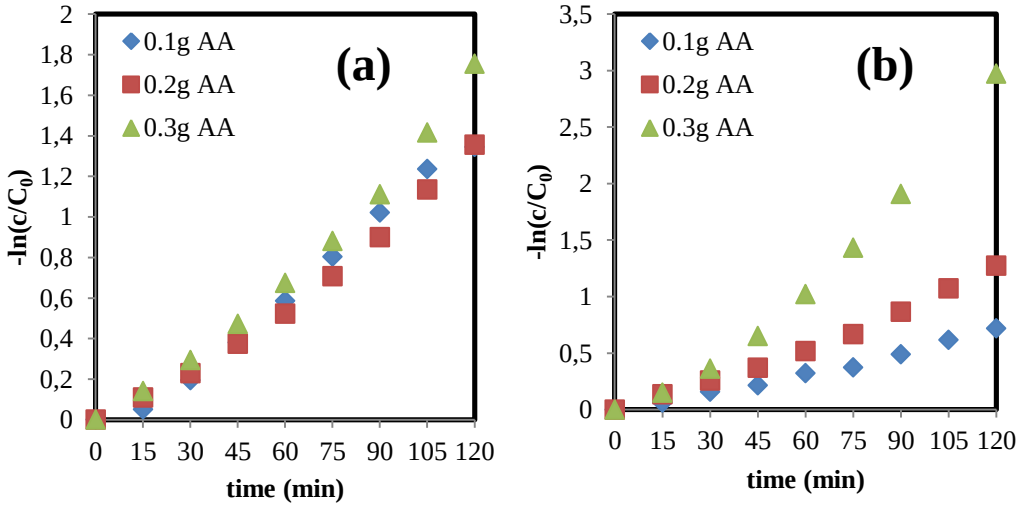

Figure 4.11: Methyl orange degradation experiment results for (a) 18g and (b) 27g PEG containing samples with 0.1g, 0.2g and 0.3g Ascorbic Acid addition.

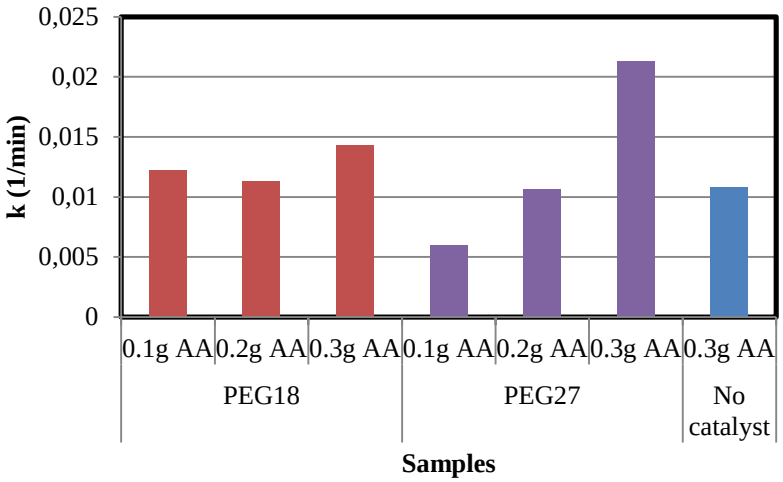

Figure 4.12: Rate constants for samples (PEG18) 18g and (PEG27) 27g PEG containing samples with 0.1g, 0.2g and 0.3g ascorbic acid (AA) addition compared with blank result with 0.3g ascorbic acid addition in the presence of no catalyst .

For both catalyst samples, the increase in the ascorbic acid amount results an increase in the reaction rate. This effect was relatively small and not firm in the smaller surface area catalyst. But the catalyst samples having higher surface, decent increase of degradation rate with increasing ascorbic acid amount was observed. When the reaction rate obtained during the blank experiment with 0.3 ascorbic acid and methyl orange in the absence of catalyst ($k=0.0108min^{-1}$) is compared with the results obtained by photocatalytic degradation in the presence of catalyst, it can be clearly stated that the presence of photocatalyst enhances the photodegradation reaction. However it is difficult to conclude on the sensitization effect of ascorbic acid on photocatalysis.

In order to ensure on the effect of ascorbic acid on photodegradation, the effect of film area on the reaction rate was also investigated. For this purpose, the photocatalytic methyl orange degradation experiments were also conducted with two thin film samples

having different sizes of 1.4cm^2 and 2.1cm^2, synthesized with 27g PEG recipe. The results of these experiments are presented in Figure 4.13..

Results show that the rate of methyl orange degradation is affected by the presence of catalyst at pH=4 and the rate of degradation slightly decreased with the increased amount of catalyst. The blank experiment performed without catalyst indicates the significant liquid phase degradation. These experiments also indicated the role of pH on methyl orange photocatalytic degradation. The results of experiments performed with thin film catalysts and solutions having different pH levels (pH=4, 7 and 10) are shown in Figure 4.14 and Figure 4.15.

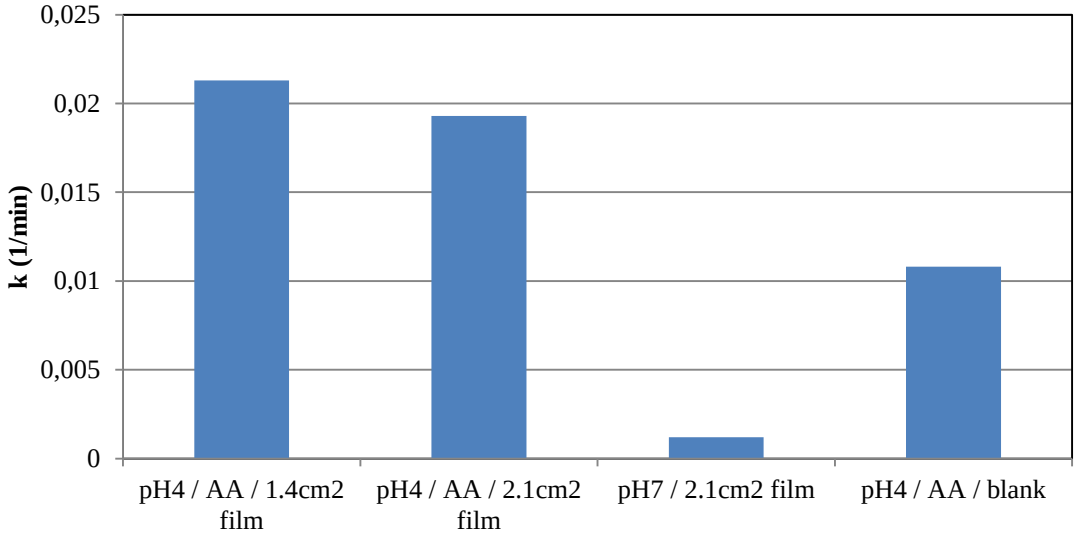

Figure 4.13: Rate constants calculated for methyl orange degradation conducted with catalyst with 1.4cm^2 film area in the presence of ascorbic acid (pH4 / AA / 1.4cm2 film), 2.1cm^2 film area in the presence of ascorbic acid (pH4 / AA / 2.1cm2 film), 2.1cm^2 film only (pH7 / 2.1cm2 film) and 0.3g ascorbic acid only (pH4 / AA/ blank).

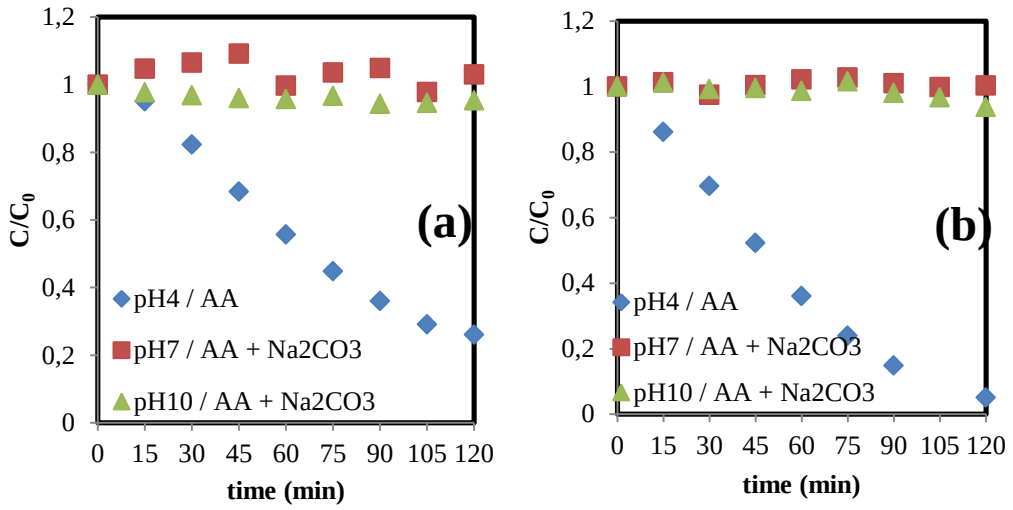

Figure 4.14: Change of concentration of methyl orange with time for (a) 18g PEG containing catalyst in 0.1g Ascorbic Acid containing solutions and (b) 27g PEG containing catalyst in 0.3g Ascorbic Acid containing solutions, for different pHs and Na2CO3 occurrences.

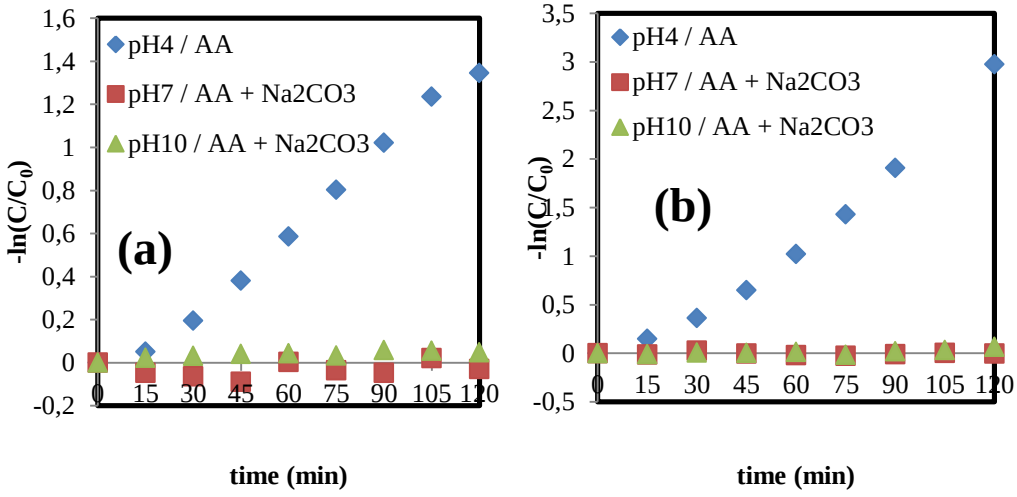

Figure 4.15: Pseudo first order behavior of photocatalytic degradation of methyl orange for (a) 18g PEG containing catalyst in 0.1g Ascorbic Acid containing solutions and (b) 27g PEG containing catalyst in 0.3g Ascorbic Acid containing solutions, for different pHs and Na_2CO_3 occurrences.

In the light of experimental results, the following reaction mechanism can be proposed for the photocatalytic degradation of methyl orange in the presence of ascorbic acid.

$A \rightarrow B\ , k_1 \quad r_1 = -k_1[A]$	Heterogeneous phase (Titanium dioxide)
$A \rightarrow B\ , k_2 \quad r_2 = -k_2[A]$	Homogenous phase (Ascorbic acid)
$A \rightarrow B\ , k_t \quad r_t = -k_t[A] = -(k_1 + k_2)[A]$	Observed reaction

Effect of pH also investigated with experiments conducted with commercial powder catalyst and methyl orange solutions having different pH levels (pH=4, 7 and 10). Two separate blank experiments without catalyst and ascorbic acid were conducted ap pH=4 and pH=7. Results are shown in Figure 4.16.

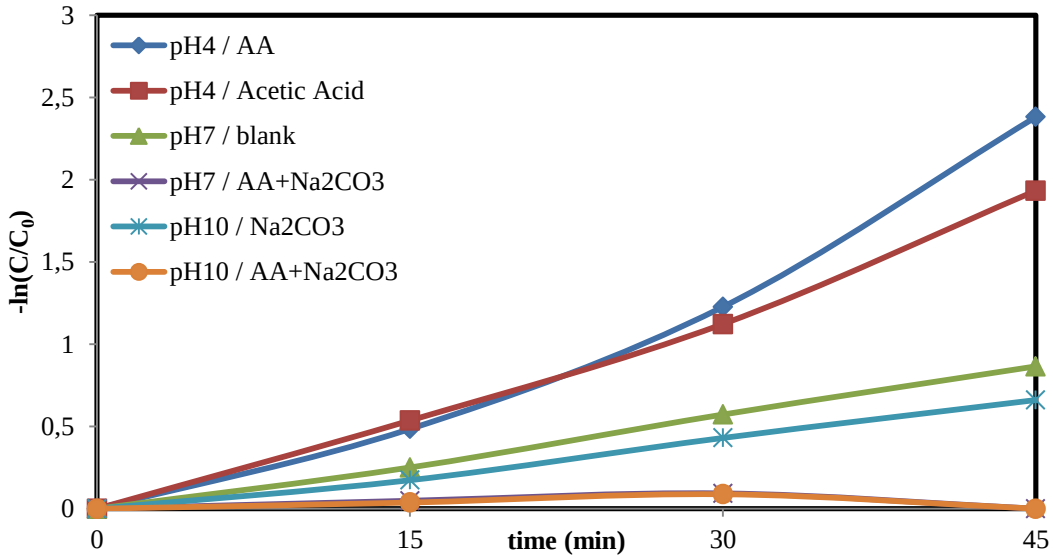

Figure 4.16: Commercial TiO2 powder experiment results.

Table 4.2: Rate constants for methyl orange degradation test over 0.4g/L commercial TiO2 powder experiments.

	pH4		pH7		pH10	
Addition	**0.3g AA**	**Acetic Acid**	**blank**	**AA+Na2CO3**	**Na2CO3**	**0.3g AA + Na2CO3**
k (1/min)	0.0526	0.0426	0.0195	-0.0015	0.0149	0

The results showed that the presence of sodium carbonate has a negative effect on the catalytic performance of TiO2. Considering pH4 and pH7 cases reported on Table 4.2 with no ascorbic acid, it might be concluded that the acidity has a positive effect on the performance of the catalyst for this reaction. The presence of ascorbic acid also increases the reaction rate constant significantly. But in the case of both ascorbic acid and sodium carbonate present in the system, the reaction is inhibited.

As a result of these activity tests conducted with catalyst and ascorbic acid, the sensitization of titanium dioxide with ascorbic acid can be explained by the following mechanism. Since adsorption of ascorbic acid on the film surface is observed under irradiation, first step should be the sensitization of titania. After the semiconductor is exited, ascorbic acid molecule interacts with the conduction band of the semiconductor and ascorbate adsorbed over the surface of catalyst [37]. This electron accepting adsorbant should be leveled 1.6eV over the valance band. [36] Explained procedure is illustrated in Figure 4.17.

Table 4.3: Effect of pH and presence of Ascorbic Acid and Sodium Carbonate of photo catalytic activity of commercial TiO2 powder

	pH 4		pH 7		pH10	
Ascorbic Acid presence	+	-	+	-	+	-
Sodium Carbonate presence	-	-	+	-	+	+
Rate constant(1/min)	0.526	0.0426	0	0.0195	0	0.0149

The effect of ascorbic acid in the reaction medium can be reported as sensitization since;

- the reaction is photocatalytic,
- sensible increase in photocatalytic activity under solar illumination for higher surface area samples was recorded,
- the effect of ascorbic acid presence is more dominant than the effect of pH, which is shown in pH4 experiments conducted with commercial titania.

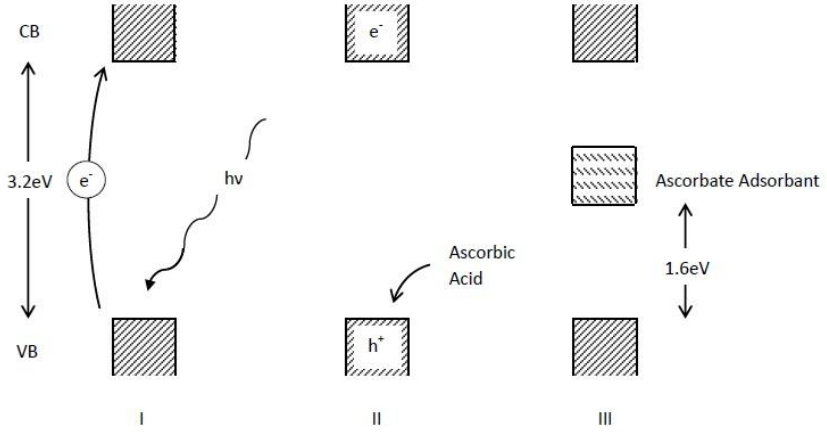

Figure 4.17: Illustration of offered mechanism for sensitization of titania with ascorbic acid.

4.3. Comparison with EDTA

Methyl orange degradation experiments showed that the photocatalytic activities of the samples are enhanced by the ascorbic acid sensitization. However, the sensitization effect should also be evidenced by comparing other sensitizers. Since ascorbic acid has antioxidant nature, which is a kind of electron donor/hole scavenger, comparison with EDTA which is a known hole scavenger for TiO2 photocatalysts [15] [20] was intended. Methyl orange degradation experiments were also repeated with EDTA replacing ascorbic acid. The results are presented in Figure 4.18. Concentration data was evaluated by the same methodology followed in the previous sections by using pseudo first order reaction approach. The results are illustrated in Figure 4.19. In the experiments conducted with presence of EDTA gas evolution and the gas film formation over the film surfaces were observed. As it is shown in the figures, limited activity was obtained with EDTA which might be attributed to the gas film formation over the surface.

In order to make a comparison, water splitting tests were conducted with EDTA by using UV irradiation. 7mL of UP grade pure water in a quartz reactor ended with a manometer was subjected to 12W of UV light at 254nm in an enclosed chamber. Level change in the manometer arm was observed to measure the gas generation in the reactor. The reactions were conducted with equimolar amounts of EDTA and compared with results obtained with ascorbic acid, with and without catalyst. Changes in manometer arm with time are presented in Figure 4.1.

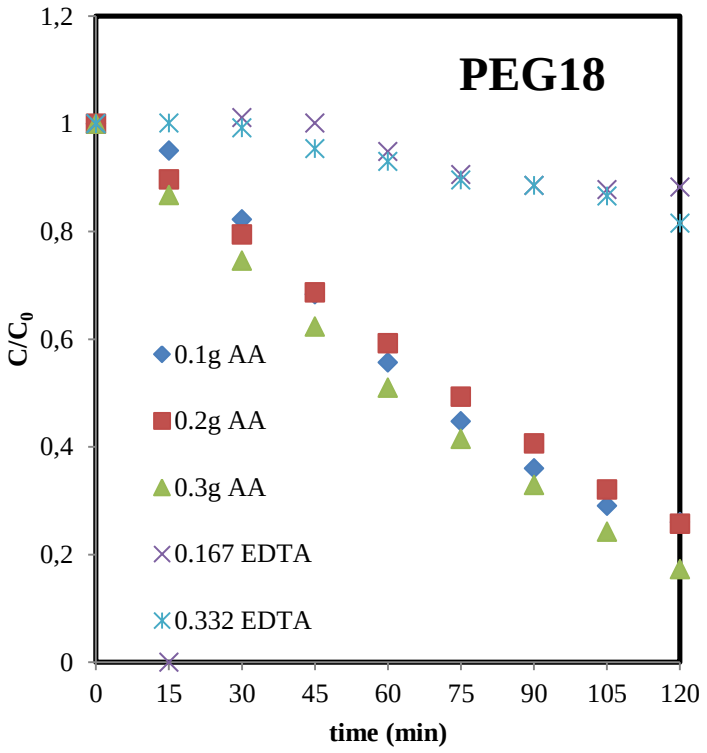

Figure 4.18: Change of concentration of methyl orange with time for different amounts of ascorbic acid and EDTA.

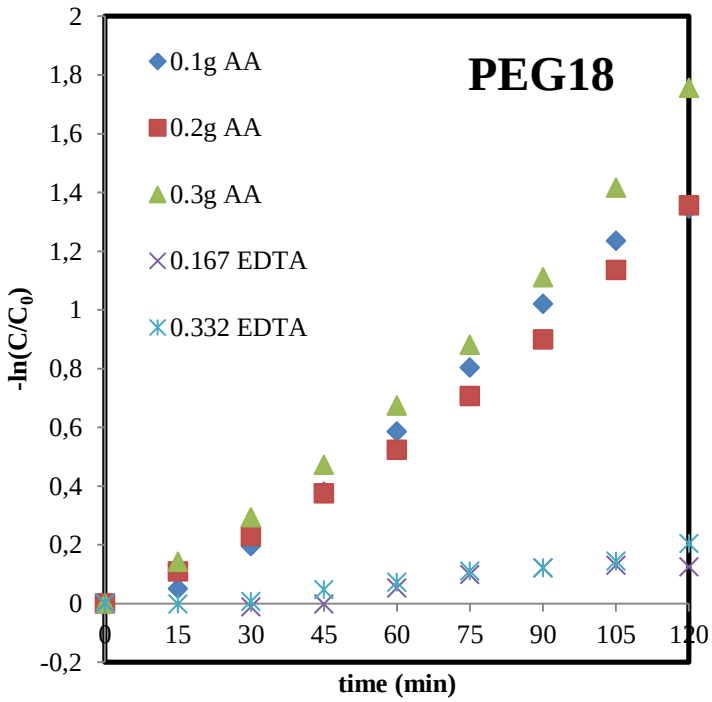

Figure 4.19: Pseudo first order behavior of photocatalytic degradation of methyl orange for different amounts of ascorbic acid and EDTA.

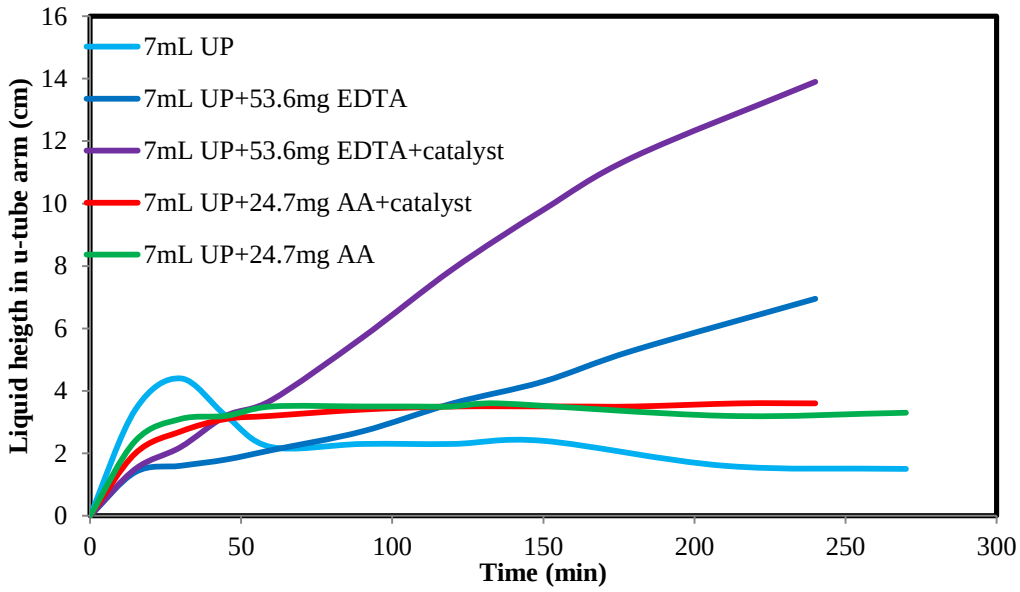

Figure 4.20: Changes of height in manometer arm with time for UV chamber experiments.

The volume of generated gas was corrected with temperature change recorded during the experiment by assuming ideal gas behavior. Calculated gas evolution rates of EDTA and AA in presence and absence of catalyst are shown in Table 4.4.

Table 4.4: Rates of gas evolution in UV chamber. (Presented in µmol/min.)

	No catalyst	**PEG27 film**
0.3mM EDTA	0.1258	0.2647
0.3mM AA	0.0009	0.0197

Results indicate the considerable gas evolution with EDTA under UV irradiation which can be explained by the decomposition of EDTA. The gas evolution rate with EDTA increases more than two folds with the presence of catalyst. On the other hand, under UV irradiation, no gas evolution was observed with ascorbic acid without catalyst. The gas evolution observed only with the presence of ascorbic acid and catalyst.

CHAPTER 5

CONCLUSIONS

- The surface area of thin films plays an important role on the photocatalytic degradation reactions.
- Ascorbic acid significantly enhances the photocatalytic activity under visible illumination. Considering the hole scavenging effect of EDTA, observed to be limited under same experimental conditions. On the other hand the effect of ascorbic acid can be called as sensitization.
- Ascorbic acid adsorption over thin SiO2-TiO2 films is the first step of sensitization and it is a photoassisted process.
- Sensitiziation by ascorbic acid requires acidic conditions. The experiments performed in the presence of ascorbic acid - sodium carbonate buffer revealed that methyl orange degradation takes place in basic and neutral conditions. However the presence of ascorbic acid inhibits the degradation under the same conditions.
- EDTA has higher hole scavenging activity for water splitting under UV illumination. This also supports the role of ascorbic acid on photocatalytic performance as sensitization in two aspects. First, the increase in activity in the presence of ascorbic acid is more pronounced with respect to EDTA under visible light. Second, under UV illumination there is no need for sensitization. In that case ascorbic acid acts as hole scavenger and its hole scavenging activity is lower than EDTA.

CHAPTER 6

RECOMANDATIONS

Having the surface area known, another important property of the films need to be investigated is pore size distribution. Diameters of the pores and tortuosity are important parameters in the aspect of adsorption.

Changes in the electronic structure of the catalyst can be investigated thoroughly. These kind of analysis gives important information of band structure and gap of semiconductor. For example XPS of the films can be investigated.

Photonic efficiency is also an important aspect in the area of sensitization. Ratios of utilized photons in the reaction to incident photons reaching to the photocatalyst in different regions electromagnetic spectrum show the activity increase and shift to visible light clearly.

Mimicking biological systems is a promising approach to overcome the problems occurring in chemical process. To follow this perspective current study can be extended with other effective antioxidants such as Vitamin E.

REFERENCES

[1] K. Köhler, P. Simmendinger, W. Roelle, W. Scholz, A. Valet and M. Slongo, "Paints and Coatings, 4. Pigments, Extenders, and Additives," in *Ullmann's Encyclopedia of Industrial Chemistry*, Wiley-VCH, 2010.

[2] S.-i. Ohkoshi, Y. Tsunobuchi, T. Matsuda, K. Hashimoto, A. Namai, F. Hakoe and H. Tokoro, "Synthesis of a metal oxide with a room-temperature photoreversible phase transition," *Nature Chemistry,* no. 2, p. 539–545, 2010.

[3] D. B. Strukov, G. S. Snider, D. R. Stewart and R. S. Williams, "The missing memristor found," *Nature,* no. 453, pp. 80-83, 2008.

[4] A. Fujishima, X. Zhang and D. A. Tryk, "TiO2 photocatalysis and related surface phenomena," *Surface Science Reports,* no. 63, pp. 515-582, 2008.

[5] S.-D. Mo and W. Y. Ching, "Electronic and optical properties of three phases of titanium dioxide: Rutile, anatase, and brookite," *Physical Review B,* vol. 51, no. 19, p. 13023–13032, 1995.

[6] W. Choi, "Pure and modified TiO2 photocatalysts and their environmental applications," *Catalysis Surveys from Asia,* vol. 10, no. 1, pp. 16-28, 2006.

[7] O. Carp, C. L. Huisman and A. Reller, "Photoinduced reactivity of titanium dioxide," *Progress in Solid State Chemistry,* vol. 32, no. 1-2, pp. 33-177, 2004.

[8] M. Çınar, Enzyme immobilization on titania-silica-gold thin films for biosensor applications and photocatalytic enzyme removal for surface patterning, MSc.Thesis Dissertation, Middle East Technical University, 2009.

[9] A. Erkan, U. Bakir and G. Karakas, "Photocatalytic microbial inactivation over Pd doped SnO2 and TiO2 films," *Journal of Photochemistry and Photobiology A: Chemistry,* no. 184, pp. 313-321, 2006.

[10] G. R. Soja and D. F. Watson, "TiO2-Catalyzed Photodegradation of Porphyrins: Mechanistic Studies and Application in Monolayer Photolithography," *Langmuir,* vol. 25, no. 9, p. 5398–5403, 2009.

[11] N. Strataki, V. Bekiari, D. I. Kondarides and P. Lianos, "Hydrogen production by photocatalytic alcohol reforming employing highly efficient nanocrystalline titania films,"

Applied Catalysis B: Environmental, no. 77, pp. 184-189, 2007.

[12] A. Fujishima and K. Honda, "Electrochemical Photolysis of Water at a Semiconductor Electrode," *Nature,* pp. 37-38, 1972.

[13] U. Diebold, "The surface science of titanium dioxide," *Surface Science Reports,* no. 48, pp. 53-229, 2003.

[14] A. J. Bard and M. A. Fox, "Artificial Photosynthesis: Solar Splitting of Water t Hydrogen and Oxygen," *Accounts of Chemical Research,* no. 28, pp. 141-145, 1995.

[15] K. Hirano, E. Suzuki, A. Ishikawa, T. Moroi, H. Shiroishi and M. Kaneko, "Sensitization of TiO2 particles by dyes to achieve H2 evolution by visible light," *Journal of Photochemistry and Photobiology A: Chemistry,* no. 136, pp. 157-161, 2000.

[16] S. U. Khan, M. Al-Shahry and W. B. Ingler Jr., "Efficient Photochemical Water Splitting by a Chemically Modified n-TiO2," *Science,* vol. 297, pp. 2243-2245, 2002.

[17] M. Kitano, K. Tsujimaru and M. Anpo, "Decomposition of water in te seperate evolution of hydrogen and oxygen using visible ligth-responsive TiO2 thin film photocatalysts: Effect of work function of te substrates on the yield of the reaction," *Applied Catalysis A: General,* no. 314, pp. 179-183, 2006.

[18] J. H. Park, S. Kim and A. J. Bard, "Novel Carbon-Doped TiO2 Nanotube Arrays with Aspect Ratios for Efficient Solar Water Splitting," *Nano Letters,* vol. 6, no. 1, pp. 24-28, 2006.

[19] J. Nowotny, T. Bak, M. Nowotny and L. Sheppard, "Titanium dioxide for solar-hydrogen I. Functional properties," *International Journal of Hydrogen Energy,* no. 32, pp. 2609-2629, 2007.

[20] M. Ni, M. K. Leung, D. Y. Leung and K. Sumathy, "A review and recent developments in photocatalytic water-splitting using TiO2 for hydrogen production," *Renewable and Sustainable Energy Reviews,* pp. 401-425, 2007.

[21] R. Dholam, N. Patel and A. Miotello, "Physically and chemically sythesized TiO2 composite thin films for hydrogen production by photcatalytic water splitting," *International Journal of Hydrogen Energy,* no. 33, pp. 6896-6903, 2008.

[22] R. Navarro, M. Sanchez-Sanchez, M. Alvarez-Galvan, F. del Valle and J. Fierro, "Hydrogen production from renewable sources: biomass and photocatalytic opportunites," *Energy and Environmental Science,* no. 2, pp. 35-54, 2008.

[23] B. Ohtani, "Photocatalysis A to Z-What we know and what we do not know in a scientific sense," *Journal of Photochemistry and Photobiology C: Photochemistry Reviews,* no. 11, pp. 157-178, 2010.

[24] A. M. Peiró, C. Colombo, G. Doyle, J. Nelson, A. Mills and J. R. Durrant, "Photochemical Reduction of Oxygen Adsorbed to Nanocrystalline TiO2 Films: A Transient Absorption and Oxygen Scavenging Study of Different TiO2 Preparations," *Journal of Physical Chemistry B,* vol. 110, no. 46, pp. 23255-23263, 2006.

[25] T. Yoshihara, R. Katoh, A. Furube, Y. Tamaki, M. Murai, K. Hara, S. Murata, H. Arakawa and M. Tachiya, "Identification of Reactive Species in Photoexcited Nanocrystalline TiO2 Films by Wide-Wavelength-Range (400−2500 nm) Transient Absorption Spectroscopy," *Journal of Physical Chemistry B,* vol. 108, no. 12, p. 3817–3823, 2004.

[26] S. G. Kumar and L. G. Devi, "Review on Modified TiO2 Photocatalysis under UV/Visible Light: Selected Results and Related Mechanisms on Interfacial Charge Carrier Transfer Dynamics," *Journal of Physical Chemistry A,* vol. 115, no. 46, pp. 13211-13241, 2011.

[27] Z. Jin, X. Zhang, G. Lu and S. Li, "Improved quantum yield for photocatalytic hydrogen generation under visible light irradiation over eosin sensitized TiO2-Investigation of different noble metal loading," *Journal of Molecular Catalysis A: Chemical,* no. 259, pp. 275-280, 2006.

[28] W. Choi, A. Termin and M. R. Hoffmann, "The Role of Metal Ion Dopants in Quantum-Sized TiO2: Correlation between Photoreactivity and Charge Carrier Recombination Dynamics," *Journal of Physical Chemistry,* vol. 98, no. 51, pp. 13669-13679, 1994.

[29] A.-W. Xu, Y. Gao and H.-Q. Liu, "The Preparation, Characterization, and their Photocatalytic Activities of Rare-Earth-Doped TiO2 Nanoparticles," *Journal of Catalysis,* vol. 207, no. 2, p. 151–157, 2002.

[30] A. A. Nada, M. H. Barakat, H. A. Hamed, N. R. Mohamed and T. N. Veziroglu, "Studies on the photocatalytic hydrogen production using suspended modified TiO2 photocatalysts," *International Journal of Hydrogen Energy,* vol. 30, no. 7, pp. 687-691, 2005.

[31] B. O'Regan and M. Gratzel, "A low-cost, high-efficiency solar cell based on dye-sensitized colloidal TiO2 films," *Nature,* vol. 353, pp. 737-740, 1991.

[32] C. J. Brinker and G. W. Scherer, Sol-Gel Science: The Physics and Chemistry of Sol-Gel Processing, San Diego: Academic Press, 1990.

[33] C. Anderson and A. J. Bard, "An Improved Photocatalyst of TiO2/SiO2 Prepared by a Sol=Gel Synthesis," *Journal of Physical Chemistry*, no. 99, pp. 9882-9885, 1995.

[34] J. Yu, X. Zhao and Q. Zhao, "Effects of surface structure on photocatalytic activity of TiO2 thin films prepared by sol-gel method," *Thin Solid Films*, no. 379, pp. 7-14, 2000.

[35] D.-O. Kim and C. Y. Lee, "Comprehensive Study on Vitamin C Equivalent Antioxidant Capacity (VCEAC) of Various Polyphenolics in Scavenging a Free Radical and its Structural Relationship," *Critical Reviews in Food Science and Nutrition*, no. 44, pp. 253-273, 2004.

[36] T. Rajh, J. M. Nedeljkovic, L. X. Chen, O. Poluektov and M. C. Thurnauer, "Improving Optical and Charge Separation Properties of Nanocrystalline TiO2 by Surface Modification with Vitamin C," *The Journal of Physical Chemistry B*, vol. 103, no. 18, pp. 3515-3519, 1999.

[37] Y. Ou, J.-D. Lin, H.-M. Zou and D.-W. Liao, "Effects of surface modification of TiO2 with ascorbic acid on photocatalytic decolorization of an azo dye reactions and mechanisms," *Journal of Molecular Catalysis A: Chemical*, no. 241, pp. 59-64, 2005.

[38] P. Qu, J. Zhao, T. Shen and H. Hidaka, "TiO2-assisted photodegradation of dyes: A study of two competitive processes in the degradation of RB in an aqueous TiO2 colloidal solution," *Journal of Molecular Catalysis A: Chemical*, no. 129, pp. 257-268, 1998.

[39] S. Kothari, A. Kumar, R. Vyas, R. Ameta and P. B. Punjabi, "Cadmium Sulfide Photocatalysed Reduction of Malachite Green by Ascorbic Acid and EDTA as Reductants," *Journal of Brazillian Chemical Society*, vol. 20, no. 10, pp. 1821-1826, 2009.

[40] X.-M. Song, J.-M. Wu and M. Yan, "Photocatalytic degradation of selected dyes by titania thin films with various nanostructures," *Thin Solid Films*, no. 517, pp. 4341-4347, 2009.

[41] S. Al-Qaradawi and S. R. Salman, "Photocatalytic degradation of methyl orange as a model compound," *Journal of Photochemistry and Photobiology A: Chemistry*, no. 148, pp. 161-168, 2002.

[42] I. K. Konstantintinou and T. A. Albanis, "TiO2-assisted photocatalytic degradation of azo dyes in aqueous solution: kinetic and mechanistic investigations A reviev," *Applied Catalysis B: Environmental*, no. 49, pp. 1-14, 2004.

[43] B. K. Erdural, A. Yurum, U. Bakir and G. Karakas, "Antimicrobial Properties of Titanium Nanoparticles," in *NATO Science for Peace and Security Series B - Physics and Biophysics*, 2008.

[44] B. Koç, Production of titanium dioxide thin films with improved photocatalytic activity: The use of bacteria as 3D templates, MSc.Thesis Dissertation, Middle East Technical University, 2009.

[45] D. W. Ball, The Basics of Spectroscopy, SPIE, 2001.

[46] A. Yürüm, The Synthesis of Titanium Dioxide Photocatalysts by Sol-Gel Method: The Effect of Hydrothermal Treatment Conditions and Use of Carbon Nanotube Template, PhD.Thesis Dissertation, Middle East Technical University, 2009.

APPENDIX A

EXPERIMENTAL DATA

Table 7.1: Raw experimental data for methyl orange degradation on PEG18 films.

	PEG18				
	pH4			pH7	pH10
t (min)	0.1g AA	0.2g AA	0.3g AA	0.1g AA + Na2CO3	0.1g AA + Na2CO3
0	0.891	0.959	1.03	0.693	0.736
15	0.847	0.86	0.894	0.726	0.719
30	0.733	0.762	0.768	0.738	0.713
45	0.609	0.659	0.642	0.757	0.707
60	0.496	0.568	0.525	0.691	0.705
75	0.399	0.473	0.427	0.718	0.712
90	0.321	0.390	0.339	0.727	0.694
105	0.259	0.308	0.250	0.678	0.696
120	0.232	0.247	0.178	0.714	0.702

Table 7.2: Raw experimental data for methyl orange degradation on PEG27 films.

	PEG27				
	pH4			pH7	pH10
t (min)	0.1g AA	0.2g AA	0.3g AA	0.3g AA + Na2CO3	0.3g AA + Na2CO3
0	0.901	0.973	1.037	0.701	0.685
15	0.848	0.850	0.893	0.710	0.693
30	0.769	0.753	0.722	0.683	0.680
45	0.727	0.672	0.542	0.704	0.682
60	0.653	0.580	0.374	0.716	0.676
75	0.620	0.499	0.248	0.720	0.696
90	0.552	0.410	0.154	0.708	0.672
105	0.486	0.333		0.700	0.662
120	0.439	0.272	0.053	0.703	0.642

Table 7.3: Raw experimental data for methyl orange degradation 2.1cm^2 film and powders.

	PEG27 (1.5x)	No cat.	0.1g TiO2					
	pH4	pH4	pH4		pH7		pH10	
t (min)	0.3g AA	0.3g AA	0.3g AA	AsAc	blank	AA+Na2CO3	Na2CO3	0.3g AA + Na2CO3
0	0.978	0.89	0.877	0.913	0.789	0.679	0.672	0.689
15	0.773	0.774	0.54	0.534	0.614	0.707	0.565	0.711
30	0.655	0.681	0.257	0.297	0.445	0.676	0.437	0.676
45	0.529	0.57	0.081	0.132	0.332	0.742	0.347	0.738
60	0.406							
75	0.296							
90	0.22							
105	0.142							
120	0.09							

Table 7.4: Results for UV chamber experiments conducted with 7mL UP

t (min)	T (oC)	h (cm)
0	13.4	0
15	28.2	3.4
30	29	4.4
45	25	3.2
60	22.2	2.2
90	22.2	2.3
120	22.1	2.3
150	22.4	2.4
210	22.4	1.6
270	22.7	1.5

Table 7.5: Results for UV chamber experiments conducted with 7mL UP+53.6mg EDTA

t (min)	T (oC)	h (cm)
0	14.5	0
15	28.3	1.4
30	28.5	1.6
45	28.2	1.8
60	27.9	2.1
90	28.2	2.7
120	28.5	3.6
150	28	4.3
180	28.8	5.3
240	28.6	6.95

Table 7.6: Results for UV chamber experiments conducted with 7mL UP+53.6mg EDTA+catalyst

t (min)	T (oC)	h (cm)
0	21.1	0
15	30.4	1.5
30	32.4	2.2
45	33.3	3.2
60	34.2	3.7
90	34.1	5.7
120	34	7.9
150	33.8	9.8
180	33.6	11.5
240	33.6	13.9

Table 7.7: Results for UV chamber experiments conducted with 7mL UP+24.7mg AA+catalyst

t (min)	T (oC)	h (cm)
0	21.3	0
15	34.2	2
30	37	2.7
45	38.2	3.1
60	39.1	3.2
90	39.3	3.4
120	39.8	3.5
159	40.1	3.5
180	39.3	3.5
215	39.3	3.6
240	39.3	3.6

Table 7.8: Results for UV chamber experiments conducted with 7mL UP+24.7mg AA

t (min)	T (oC)	h (cm)
0	21.5	0
15	24.8	2.4
30	35.2	3.1
45	34.8	3.2
60	37.3	3.5
90	37.4	3.5
105	37.5	3.5
120	36.3	3.5
135	33.4	3.6
210	33.9	3.2
270	33.6	3.3

APPENDIX B

UV-VIS CALIBRATION CURVE

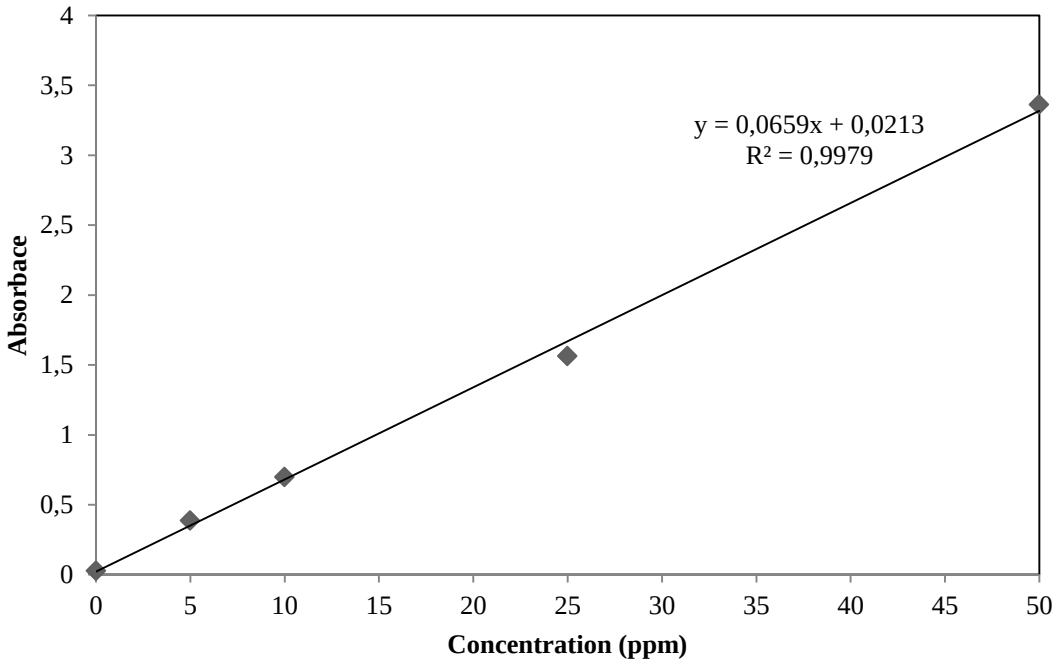

Figure 8.1: UV-Vis Spectrophotometer absorbance results for 499nm wavelength light for changing concentrations of MO in aqueous solution.

APPENDIX C

SUNTEST SPECTRUM

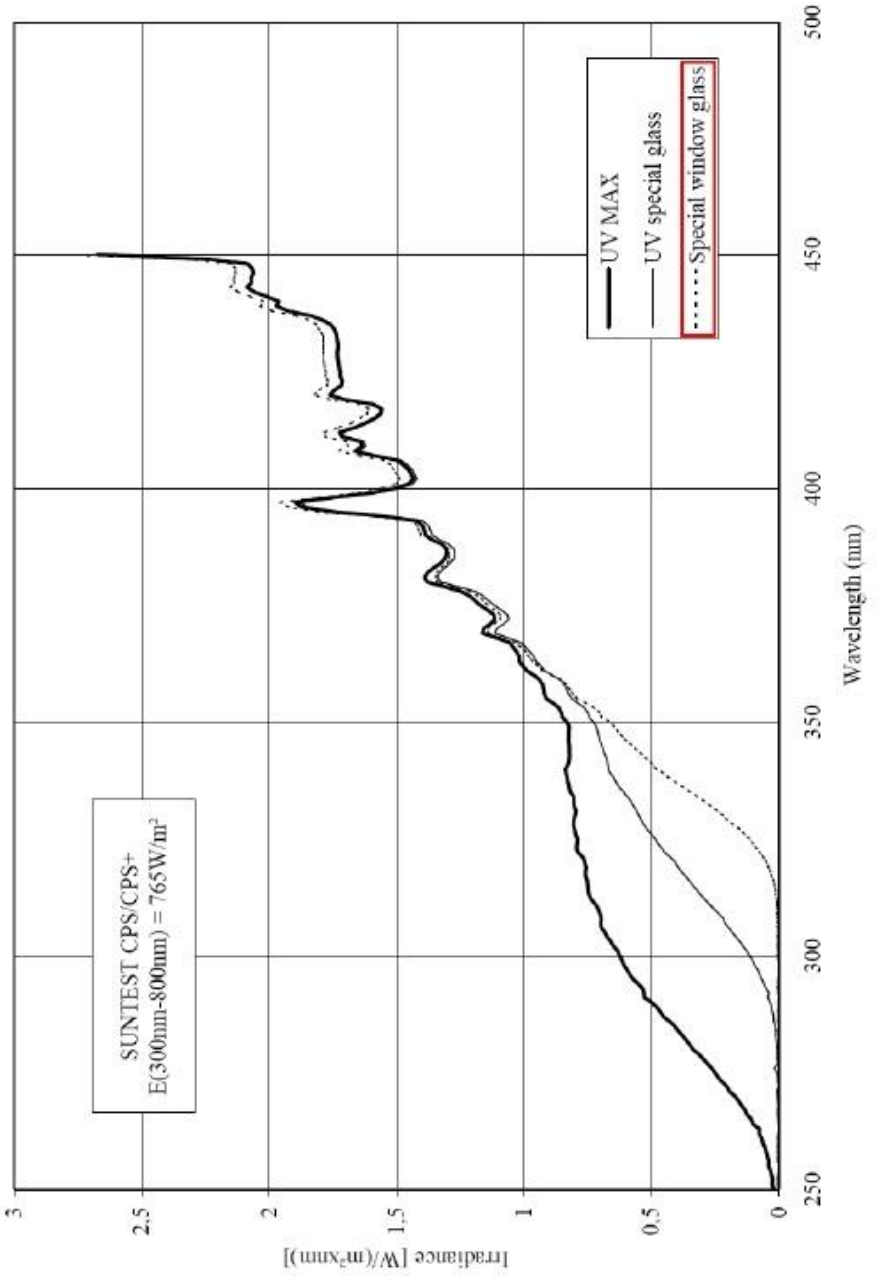

Figure A.1: Illumination spectrum for ATLAS SUNTEST CPS+ device. [46]

APPENDIX D

SURFACE AREA CALCULATIONS

PEG10

Table 9.1: Data required for surface area calculation of 10g PEG containing sample.

Ci (ppm)	m (g)	S glass (cm2)	Abs.	Ce	x	x/m	Ce/(x/m)
1	1.4187	10.54492771	0.153	0.674009	0.00652	0.000618	1090.118
2	1.4051	10.44384149	0.342	1.486957	0.010261	0.000982	1513.472
4	1.4469	10.75453296	0.737	3.338618	0.013228	0.00123	2714.415

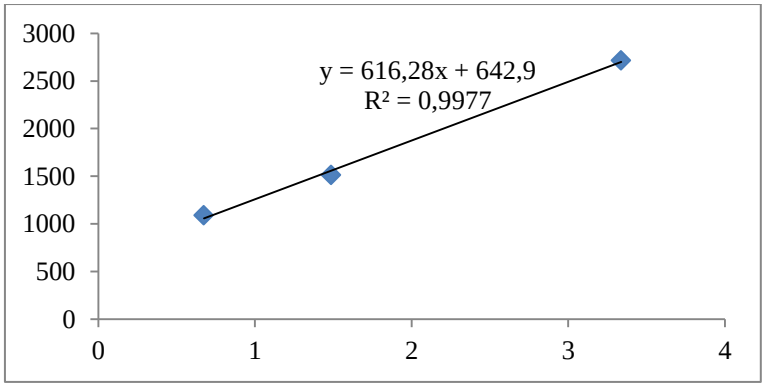

Figure 9.1: Adsorption isotherm for 10g PEG containing sample.

Table 9.2: Monolayer adsorption capacity and relative surface area for 10g PEG containing sample.

1/xm	xm	S (cm2/cm2)
616.28	0.001623	31.35048026

PEG18

Table 9.3: Data required for surface area calculation of 18g PEG containing sample.

Ci (ppm)	m (g)	S glass (cm2)	Abs.	Ce	x	x/m	Ce/(x/m)
1	1.3034	9.687924705	0.088	0.387665	0.012247	0.001264	306.6681
2	1.2807	9.519199915	0.26	1.130435	0.017391	0.001827	618.748
4	1.3124	9.754819996	0.69	3.125708	0.017486	0.001793	1743.737

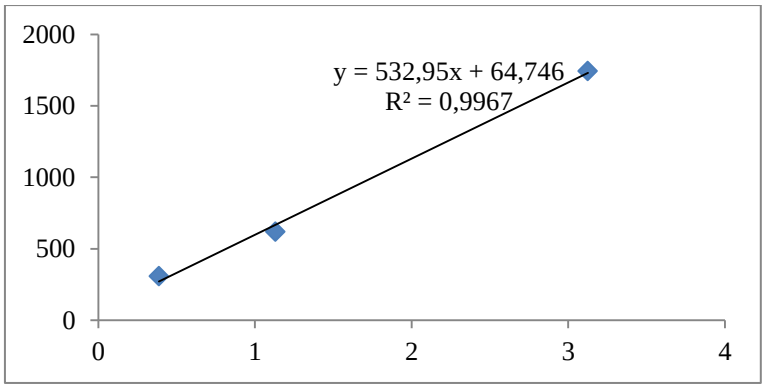

Figure 9.2: Adsorption isotherm for 18g PEG containing sample.

Table 9.4: Monolayer adsorption capacity and relative surface area for 18g PEG containing sample.

1/xm	xm	S (cm2/cm2)
532.95	0.001876	36.25232006

PEG27

Table 9.5: Data required for surface area calculation of 27g PEG containing sample.

Ci (ppm)	m (g)	S glass (cm2)	Abs.	Ce	x	x/m	Ce/(x/m)
1	1.3307	10.43707072	0.096	0.422907	0.011542	0.001106	382.427
2	1.3738	10.77511667	0.24	1.043478	0.01913	0.001775	587.7336
4	1.3067	10.27606633	0.655	2.967157	0.020657	0.00201	1476.058

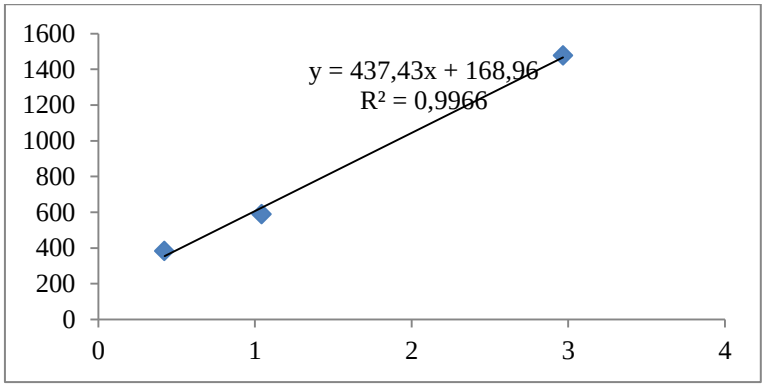

Figure 9.3: Adsorption isotherm for 27g PEG containing sample.

Table 9.6: Monolayer adsorption capacity and relative surface area for 27g PEG containing sample.

1/xm	xm	S (cm2/cm2)
437.43	0.002286	44.1686075

PEG40

Table 9.7: Data required for surface area calculation of 40g PEG containing sample.

Ci (ppm)	m (g)	S glass (cm2)	Abs.	Ce	x	x/m	Ce/(x/m)
1	1.3268	10.55241528	0.16	0.704846	0.005903	0.000559	1259.99
2	1.3379	10.64069672	0.34	1.478261	0.010435	0.000981	1507.432
4	1.3287	10.47209291	0.764	3.460929	0.010781	0.00103	3361.63

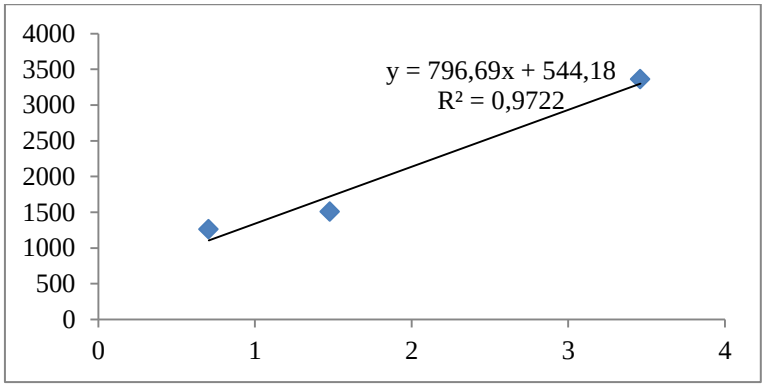

Figure 9.4: Adsorption isotherm for 40g PEG containing sample.

Table 9.8: Monolayer adsorption capacity and relative surface area for 40g PEG containing sample.

1/xm	xm	S (cm2/cm2)
796.69	0.001255	24.25118174